Ectodermal Origin and Tissue Dedifferentiation in the Podocyst Production by the Polyps of the Asian Moon Jelly (*Aurelia coerulea*)

*Hideki Ikeda

Abstract

The podocyst of *Aurelia coerulea* is derived exclusively from the ectoderm in the pedal disc and stalk of polyps. The pedal disc of the polyp expands with the involvement of stalk ectodermal cells, and the pedal disc ectoderm then invaginates to form a cyst capsule and nutrient granules and undergoes dedifferentiation. Finally, these cells are radially arranged with the formation of extracellular matrix and closure of the capsule to become a podocyst.

Pedal-disc expansion stage

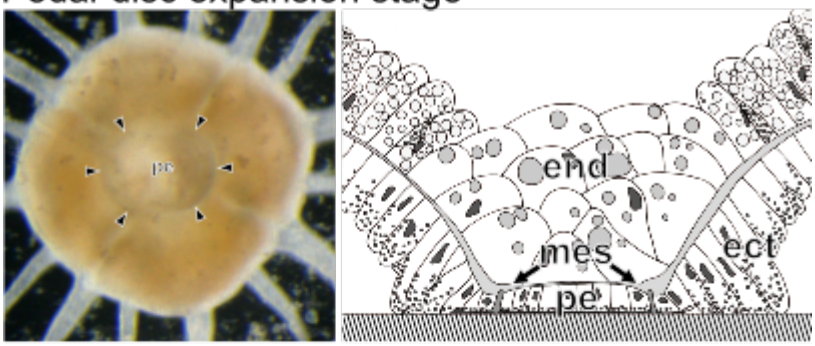

Capsule-forming stage

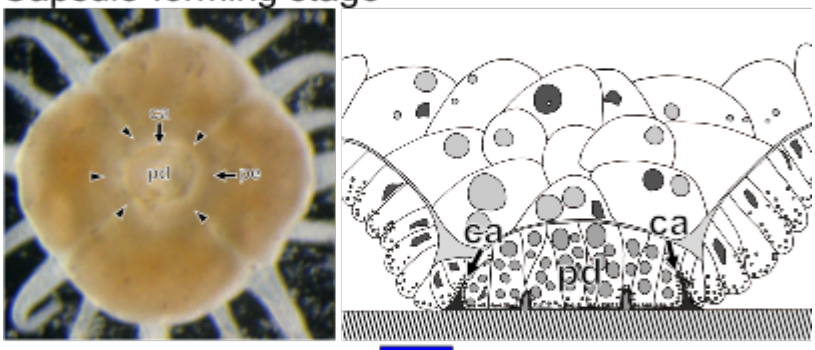

Capsule-tanning stage

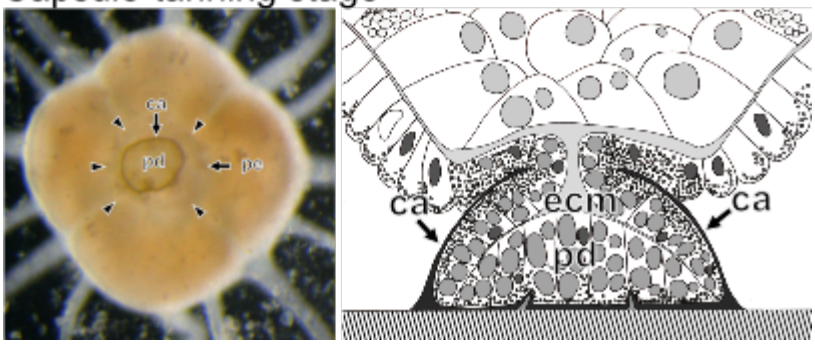

Ectodermal Origin and Tissue Dedifferentiation in the Podocyst Production by the Polyps of the Asian Moon Jelly (*Aurelia coerulea*)

Hideki Ikeda

Graduate School of Integrated Science for Life, Hiroshima University

4-4, 1-chome, Kagamiyama, Higashi-Hiroshima 739-8528, Japan

Email: hydekid3@gmail.com

ORCID ID: 0000-0002-8012-9933

Abstract

Histological origin of podocysts in scyphozoans has long been undetermined, with uncertainty whether they arise from mesenchymal amoebocytes or stalk and pedal disc ectoderm in polyps, due to the difficulty of histological investigation on the pedal disc/substrate boundary. In this study, we investigated the histological characteristics of polyps during podocyst production in Asian moon jelly (*Aurelia coerulea*) with utilizing those attached on thin polystyrene substrates that can be decomposed in histological processing, enabling fine histological observations at the pedal disc/substrate boundary. Our findings unequivocally demonstrate that the cell mass of podocysts originates from the ectoderm of the pedal disc and the stalk without the involvement of amoebocytes in the mesoglea. Preceding the podocyst formation, the pedal disc undergoes enlargement facilitated by the elongated stalk ectodermal cells, which attach to a substrate. Subsequently, the pedal disc ectoderm give rise to the primary podocyst cells with accumulating nutrient granules in the cytoplasm and forming the cyst capsule cooperatively with the invaginated pedal disc ectoderm. Direct transformation from the ectodermal cells to podocyst cells suggests that podocyst formation involves tissue dedifferentiation. Throughout the period of podocyst production, the gastrodermis of polyps is physically separated from the ectoderm with the mesoglea and shows no histological changes, and no amoebocytes appeared in the mesoglea. These histological properties are totally different from those in other modes of asexual reproduction, which incorporate the endoderm of polyps, suggesting the developmental and evolutionary differences between these asexual reproductions and podocyst production in Scyphozoa.

Research Highlights

1. The exclusive ectodermal origin of the cellular components within the podocysts of the Asian moon jelly, Aurelia coerulea.
2. The collaborative construction of the podocyst capsule by podocyst cells and ectodermal cells undergoing transformation into podocyst cells.
3. The unique podocyst production mechanism, distinct from other modes of asexual reproduction and dormant forms in Scyphozoa, indicating an independent evolutionary development within the Scyphozoa lineage.

Keywords: asexual reproduction, dormancy, Scyphozoa, pedal disc, stalk, mesoglea, cyst capsule

1. Introduction

Polyps of scyphozoan jellyfishes serve as the hub of their life cycle and undergo asexual reproduction in various manners with different ecological roles (Lucas et al., 2012). The formation of polyp buds on the lateral calyx or the extended stolon results in a rapid and efficient polyp cloning (Han & Uye, 2010). The release of planuloid buds from the ectoderm of the lateral calyx or the endoderm of polyps is used for population dispersal as an analogue of planula formation by medusae (Heins et al., 2015; Vagelli, 2007). The formation of encapsulated cell masses, called podocysts, serves both asexual reproduction and dormancy (Arai, 2009). Benthic populations built up by these reproductions undergo strobilation to release ephyrae that develop into medusae (Arai, 1997). The ecophysiological aspects of these asexual reproductions, including the effect of physicochemical and biological environments and the interrelationship among these modes, have been well documented for the increasing jellyfish problems in worldwide marine ecosystems (Rato et al., 2021; Treible & Condon, 2019; Widmer et al., 2016), while their histological and developmental mechanisms have received less attention (D. M. Chapman, 1968; Hofmann & Honegger, 1990).

Among these asexual reproductive modes, podocysts are a distinguished asexual reproduction in conduct of long dormancy, degeneration of tissue into anaplastic cell mass and the formation of chitinous capsule in the Class Scyphozoa, especially in the Order Discomedusae (Arai, 2009). In 37 discomedusan species whose life cycle has been revealed, 27 species (73%) have podocysts in their life cycle, manifesting their ecological importance in this group (Appendix 1). Formation (encystment) is influenced by various environmental conditions, such as food availability, temperature and salinity

(Thein et al., 2012, 2013; Widmer et al., 2016). Podocysts are capable of keeping dormant over years, and the longest record of dormant duration is 6 years exhibited by the podocysts of *Nemopilema nomurai* (Kawahara et al., 2013). Furthermore, they have a strong resistance to unfavorable environments, such as predation, microbial attacks and hypoxia (Kawahara et al., 2013; Takao et al., 2014). The excystment is triggered by seasonal temperature increase or decrease, high salinity and the hypoxia followed by reoxygenation (Kawahara et al., 2013; Thein et al., 2012, 2013). These ecophysiological characters facilitate them in population dynamics of species in fluctuated environments, even with artificial perturbations (Dawson & Hamner, 2009; Thein et al., 2013).

Morphological characters of podocysts have been investigated in several studies. Podocysts are generally formed beneath the pedal disc of polyps in all species, and are occasionally observed at the distal ends of extended stolons in *Aurelia* spp. (D. M. Chapman, 1968; Scorrano et al., 2017; Thein et al., 2012), *Catostylus mosaicus* (Pitt, 2000), *Chrysaora chesapeakei* (formerly identified as *C. quinquecirrha*) (Cargo & Rabenold, 1980), *Rhizostoma pulmo* (Fuentes et al., 2011), *Rhopilema nomadica* (Lotan et al., 1992) and *Rhopilema verrilli* (Calder, 1973). In both styles, podocysts consist of a mass of anaplastic cells filled by many intracellular granules (1–10 μm in diameter) containing protein, polysaccharides and lipids, and enclosed in a chitinous capsule having approximately 10 μm in thickness, with 200–500 μm in base diameter (Black, 1981; Blanquet, 1972; D. M. Chapman, 1968). Upon excystment, podocysts dissolve the upper part of the capsule with enzymatic secretion and emerge from the opening with developing into polyps, tracing the process of embryonic and larval development (Black et al., 1976; Ikeda et al., 2011a).

Histological process of podocyst formation have preliminary been investigated

since ca. 100 years ago by Hadži (1912) and Hérouard (1912) but is still incompletely understood. Because the polyps settle on a hard substrate, histological analysis on the pedal disc, where the podocysts are produced, is difficult without tissue injuries (Mayorova et al., 2012). Up to date, two contradictory hypotheses for the origin of podocysts have been argued. One is "mesoderm origin hypothesis" proposed by Hérouard (1912) and Chapman (1968) based on the observations of podocyst production by the polyps of *Chrysaora* sp. and *Aurelia aurita*, arguing that the amoebocytes in the mesenterial mesoglea of these polyps gather to form a cell mass, which moves to the beneath of the pedal disk and develop into a podocyst. Another hypothesis is "ectoderm origin" proposed by Chapman (1970a) and Magnusen (1980) based on the observation of the podocysts of *A. aurita* and *Chrysaora chesapeakei*, demonstrating that the podocysts are formed by means of the laceration of the pedal disc ectoderm from the stolon of polyps. The origin of podocysts is a key to understand the processes of the cell differentiation upon making asexual propagation and the subsequent regeneration of individual polyps, which generate medusae conducting sexual reproduction (Arai, 1997).

This study investigated the histological process of the podocyst formation in the Asian moon jelly *Aurelia coerulea*, whose polyps produce podocysts under low food availability (Thein et al., 2012), to reveal the origin of the cell mass and the capsule. To overcome the difficulty of observing the pedal disc of podocyst-producing polyps, we selected substrates that did not inhibit the process of histological analysis. First, the changes in the external morphology of polyps during podocyst production were examined and classified into 4 stages. The histochemical characteristics of polyps at each stage were examined. Finally, the histological origin of podocysts is demonstrated

by comparison with the previous hypotheses, and the developmental and evolutionary characteristics are elucidated by comparison with other asexual reproduction and dormancy in Scyphozoa.

2. Materials and methods

Preparation of polyps

Stock polyps of *Aurelia coerulea* von Lendenfeld, 1884 (Scyphozoa, Discomedusae) were established from planulae collected in Tashima, Fukuyama, located in the middle Inland Sea of Japan, in 2020. These planulae were kept in plastic containers (13 cm in diameter, 5 cm in height) containing 200 ml of filtered seawater at 22°C and salinity 33 in darkness, which were also applied to the maintenance of the developed polyps throughout this work. After the settlement of planulae, the developed polyps (ca. 100 polyps per container) were fed with newly hatched *Artemia* nauplii (ca. 500 ind. per container) once per week, and the water was exchanged on the following day. Polyps having >16 tentacles were detached from the bottom of the containers, and 3-5 polyps were placed in 5-ml culture dishes (5 cm in diameter) with a thin transparent polystyrene sheet (0.2 mm in thickness and 5 cm in diameter) at the bottom and 3 ml of seawater. Polystyrene is a suitable material for the attachment of scyphozoan polyps (Hoover & Purcell, 2009). After settling on the sheet, the polyps were transferred to13-cm container, along with the culture dish and sheet, and fed with 1–3 newly-hatched *Artemia* nauplii per polyps once a week to promote podocyst production (Thein et al., 2012). For the daily observation of morphological changes with podocyst formation, the polyps were turned over together with the substrate sheets and the underside was

photographed under a stereoscope (Olympus SZ10) equipped with a digital camera (Olympus DP20).

Histochemical analysis

Polyps were picked up with cutting the substrate sheet into a small piece (ca. 2–3 mm^2) at various timing of podocyst production. These polyps were fixed with 4% formaldehyde in 0.1 M HEPES buffer (pH 7.4) at 20°C within a week. For detecting lipids, the specimens were first fixed 2% formaldehyde and 2.5% glutaraldehyde in 0.1 M HEPES buffer (pH 7.4) at 20°C for a week and then with 2% osmium tetraoxide in 0.1 M phosphate buffer (pH 7.4) for 2 h on ice. The fixed specimens were dehydrated with ethanol solutions, with the concentration increasing from 50% to 100%. Thereafter, these samples were immersed in pure methyl methacrylate or propylene oxide for both dissolvement of the substrate polystyrene sheets and further dehydration of tissues. These dehydrated specimens were embedded in Technovit 7100 resin or Spurr epoxy resin poured into polyethylene capsules and polymerized at 60°C. These embedded specimens were sectioned at 1 μm in thickness using a glass knife on Reica EM UC6rt ultramicrotome and mounted on glass slides. Before staining, sections of epoxy resin embedded specimens were immersed in 2% KOH in ethanol for resin removal (Imai et al., 1968). These sections were subjected to various histochemical staining such as hematoxylin and eosin (HE), HE with Victoria blue (HEVB), iron eriochrome cyanin R (Fe-ECR), periodate acid Shiff (PAS) and toluidine blue (TB) (D. M. Chapman, 1968; Stefanović et al., 2015; Yamaguchi et al., 2000). Stained specimens were covered by a glass slip and examined under a light microscope (Olympus BH10) with a digital camera (Canon EOS Kiss X3).

3. Results

Changes in the external morphology of *A. coerulea* polyps during podocyst formation

When18 mature polyps of *Aurelia coerulea* (mean calyx diameter: 1.1 mm, SD: 0.22 mm) were observed over 3 months with a feeding regime of 3 *Artemia* nauplii polyp^{-1} week^{-1}, 11 of them formed a total of 20 podocysts, having 285 μm in mean long base axis, with the average production of 1.6 podocysts polyp^{-1}. All podocysts were formed beneath the pedal disc of the parental polyps, not at the distal ends of their extended stolons, although the polyps actively extended their stolons to wander on the substrates during the observation period (Fig. 1). The process of podocyst production in each polyp progressed sequential or partially overlapped, with no more than two podocysts produced simultaneously by a polyp. Only two polyps performed stolon budding, each producing one polyp.

Based on the external morphology of the polyps, we categorized the process of podocyst formation into 4 stages: 1) pre-production stage, 2) pedal disc expansion stage, 3) capsule-forming stage and 4) capsule-tanning stage. In the pre-production stage, polyps typically have a very short stalk (approximately 40 μm in length) and a small and round pedal disc with approximately 200 μm in diameter (range: 93–310 μm) (Fig. 1A). Polyps sometimes extend additional stolons from the center of the bottom calyx. The pedal disc attaches to the substrate with intermittent chitinous pedal cuticle, occasionally tanning to be pale brown in color particularly on the edge (Fig. 1A).

In the pedal-disc expansion stage, the pedal disc of the main stalk expands to reach an area of 490–890 μm in diameter (Fig. 1B). The enlargement of pedal disc took

2–3 days. The pedal cuticle disappeared with the enlargement of pedal disc. The tissue underneath the pedal disc remains homogenous, showing no signs of tissue differentiation until the next stage.

The third stage, capsule-forming stage, commences about 1 days after the pedal disc enlargement. The entire podocyst base is formed uniformly without any specific directionality, such as from center to edge. The podocyst base exhibits a pale brown color resembling the pedal cuticle and measures 210–380 μm in long axis (Fig. 1C). The base area of the capsule occupied 10–53% (mean: 26%) of that of the pedal disc the parental polyps (Fig. 1C).

In the fourth stage, capsule-tanning stage, the color of the podocyst base becomes dark brown, especially at the periphery (Fig. 1D). Internal change of the formed podocyst is not observable from the outside. Subsequently, the parental polyps form a new pedal disc near or far from the podocyst, maintaining contact by extending the original stalk. They then retract the extending stalk to move away from the completed podocyst. Throughout this process of podocyst formation, no significant morphological changes appear in the calyx of polyps (Fig. 1).

Histological changes during podocyst formation

Polyps embedded in the two types of resin after the removal of the styrene substrate plates were observed in histological and histochemical analyses without significant artefacts. A total of 81 polyps were observed, consisting of 34 polyps in pre-production stage, 31 in pedal disc expansion stage, 6 in capsule-forming stage and 10 in capsule-tanning stage. The polyps show unique histological characteristics in each stage of podocyst formation.

Pre-production stage

Pre-production stage represents a pausal period in podocyst production and shows the basic structure of the ectoderm, endoderm and the extracellular matrix, the mesoglea, in polyps. The ectoderm is composed of a single layer of columnar ectodermal cells, except in the interradial septa where the cells invade the bottom of the calyx in a random arrangement and form septal muscles (Fig. 2A, B). The histological characteristics of ectodermal cells varies depending on their location in the polyp. From the manubrium to the lateral calyx, the cells have a relatively low height (7–35 μm), large vacuoles (Fig. 2A, B). Cnidocytes are dense in the tentacles and sparse in the calyx and the manubrium (Fig. 2B). From the bottom calyx to the stalk, the ectodermal cells are relatively tall (20–50 μm in height) and have many small protein vesicles that stain red in Fe-ECR test (approximately 1 μm in diameter) (Fig. 2A, C). In the bottom of the pedal disc, relatively small cubic cells (approximately 10 μm in height and width) are located and are characterized by small number of protein vesicles (Fig. 2C). No other cell types, including nematocytes, are observed. An amorphous pedal cuticle surrounds the stalk and the underside of pedal disc, intervening between the pedal disc and the substrate (Fig. 2C). Short fiber bundles (20 μm long, 5 μm thick), forming rivet-like structures, penetrate the ectoderm of the pedal disc and connect between the mesoglea and the pedal cuticle, anchoring the polyp to the substrate (Fig. 2C).

Endoderm can be divided into four distinct subcomponents based on cellular morphology. The scyphopharyngeal endoderm lines the inner surfaces of the manubrium and the oral disc and consists of columnar cnidocytes and secretory cells (Fig. 2B, D). The tenticular endoderm is comprised of vacuolated cells filling the

interior of the tentacles (Fig. 2B). The gastrovascular endoderm is distributed within the gastrovascular cavity from the uppermost region to the middle of the base of the calyx and is characterized by numerous adipose cells, which possess many lipid granules that are stained pale white in the TB test, and a lesser number of secretory cells possessing secretory vesicles (Fig. 2B). The aboral bulge endoderm, where vacuolated endodermal cells are stacked, extends from the center of the calyx to the pedal disc within the gastrovascular cavity and protrudes toward the scyphopharynx (Fig. 2A, C).

A mesoglea lies between the ectoderm and endoderm, except at the tip of the manubrium where these two layers merge (Fig. 2B, C, D). The thickness of the mesoglea is highly variable. Typical thickness is 0.5–2.5 μm in the calyx, but thickness can increase to over 20 μm in the stalk and manubrium (Fig. 2B, C, D). No cells are present within the mesoglea throughout the polyp body (Fig. 2B, D).

Pedal disc expansion stage

As the expansion of pedal disc progresses, the histological structure of polyps gradually changes. The stalk ectodermal cells elongate themselves to attach to the substrate outside the pedal disc, joining to the enlargement of the disc (Fig. 3A, B). These cells maintain small vesicles in their cytoplasm (Fig. 3B). The cells of the original pedal disc maintain their size and shape and do not accumulate nutrient materials in their cytoplasm (Fig. 3B). The pedal cuticle and rivets remain beneath the original pedal disc, but the peripheral cuticle ridge is reduced.

Insignificant histochemical changes occur in the endodermal cells of the aboral bulge above the pedal disc, as well as in all the cellular tissues of the other parts of the polyp body. In contrast, the mesogleal layer of stalk is pulled and bent obliquely

downward by the attached ectodermal cells (Fig. 3B).

Capsule-forming stage

Histologically, the capsule-forming stage is further divided into two sub-stages: early and late stages. In the early stage, the pedal disc ectodermal cells transform into primary podocyst cells and initiate the formation of the podocyst capsule. In the central region of the pedal disc, the ectodermal cells increase in height to 30–50 μm and form a dome-shaped clump that elevates the upper mesoglea (Fig. 4A). Simultaneously, these cells deposit relatively large intracellular granules (1.5–6 μm in diameter) containing protein, exhibiting a red reaction in the Fe-ECR test, and polysaccharides, displaying a moderate purple reaction in the PAS test, in their cytoplasm (Fig. 4A, B), giving rise to a primary podocyst cells. In the outer region of the clump, the ectodermal cells with small vesicles, stained dark red in the Fe-ECR test, invaginate upwards, leading to the formation of a podocyst capsule within the interspace of the invagination (Fig. 4C). Beneath the pedal disc including the primary podocyst cells, a new pedal cuticle is formed (Fig. 4C). At the corner of the pedal disc, new anchorages are established between the pedal cuticle and the mesoglea via rivets, with the mesoglea swelling to a thickness of 9–60 μm (Fig. 4A).

In the late stage, the primary podocyst cells continue to grow to ca. 100 μm in height and deposit granules (Fig. 5A). The pedal disc ectoderm continues to invaginate towards the center of the stalk of the polyps, forming the podocyst capsule (Fig. 5B). In the inner side of the invaded ectoderm, inside the podocyst, the ectodermal cells gradually deposit protein- and polysaccharide-containing granules in the cytoplasm and transform into podocyst cells (Fig. 5B, C).

Throughout the capsule-forming stage, the mesoglea of the pedal disc maintains the physically separation between the ectoderm, including the podocyst cells, and the endoderm (Fig. 4A, 5A). The podocyst cells maintain tissue continuity with the adjacent pedal disc ectoderm (Fig. 4A). No cells were observed moving within the mesoglea and invading the pedal disc. No significant histological changes occur in the endoderm immediately above the podocyst cells (Fig. 4A, 5A).

Capsule-tanning stage

In the capsule-tanning stage, the capsule formation and tissue changes progress to complete the podocyst formation (Fig. 6A). This stage is histologically characterized by the formation of extracellular matrix inside the podocyst. In the early stage, many fibers of extracellular matrix extend continuing from the mesoglea to the podocyst cells in the central area of the podocysts (Fig. 6A, B). The podocyst cells located in the central region move down towards the bottom of the podocyst, decreasing in height, while those in the peripheral region move towards the top of the podocyst, forming the cyst capsule (Fig. 6B). These cell movements result in a radial arrangement of the cells within the podocyst in the late stage (Fig. 6A). The small protein vesicles are reduced in the stalk ectoderm, whereas they are preserved in the podocyst cells, especially around the tip of the closing capsule (Fig. 6C). The lateral plate of the capsule become thicker before the closing capsule (Fig. 6C). As the completion of podocyst formation approaches, the invaginating ectoderm approaches to reassemble each other (Fig. 6C). In addition, the ectoderm at the margin of pedal disc is detached from the substrate and lifted onto the capsule of podocysts (Fig. 6A).

After the closure of the capsule, the parental polyps detach from the podocyst with

the formation of a new pedal disc at the near or far position (Fig. 7A). The completed podocyst is filled with granules containing proteins and polysaccharides, and the extracellular matrix has disappeared from the cell mass (Fig. 7B, C).

4. Discussion

We examined the histological process in the podocyst formation of the polyps of *Aurelia coerulea* using histochemical techniques involving the dissolution of polystyrene substrates attached by polyps with organic solvents (propylene oxide and methyl methacrylate). Our procedures of embedding and sectioning of specimens can be carried out without significant obstruction. Previous work has used a cuticular tunic of tunicates or live brown algae *Laminaria* as a substratum of polyps for histological studies (D. M. Chapman, 1968, 1970a), but these materials present difficulties in sample observation. The alternative transparent polystyrene sheet is readily available and manageable, making it easy to observe the boundary between a substrate and the attachment tissues of sessile animals. Integrated with the plastic embedding, our methods can provide high-resolution histological images of scyphozoan polyps, revealing the previously unclear histological features in the podocyst production.

Cellular origin of podocysts

The process of the podocyst formation in *A. coerulea* can be summarized in Fig. 8 as follows: 1) a polyp stands on substrates with a small pedal disc and a stalk, facilitated by the intervention of a pedal cuticle before podocyst production (Fig. 8A), 2) stalk ectodermal cells elongate towards the substrate, joining to the pedal disc and expanding

the pedal disc to establish the field of podocyst formation (Fig. 8B), 3) primary podocyst cells emerge in the central area of the pedal disc, elongating themselves and depositing nutrient granules (Fig. 8C), 4) the ectodermal layer of the pedal disc invaginate inward of the polyp stalk, forming the podocyst capsule and transforming into podocyst cells (Fig. 8D), 5) podocyst cells are housed inside the capsule with forming the extracellular matrix and arranged radially to be enclosed within the capsule (Fig. 8E) and 6) the parental polyps detach from the completed podocysts (Fig. 8F).

Our histological findings indicate that the podocysts of *A. coerulea* originate exclusively from the ectodermal cells of the polyp pedal disc and stalk, as evidenced by the *de novo* emergence of podocyst cells within the pedal disc ectoderm, the continuity of ectoderm from the stalk to the podocyst cells and the absence of the breakage in the pedal disc mesoglea throughout podocyst production (Fig. 3, 4, 5). These results support the hypothesis of Magnusen (1980), as well as a part of Chapman (1970a), that the podocysts exclusively originate the ectoderm. On the contrary, the hypothesis of Hérouard (1912) and Chapman (1968), suggesting that the amoebocyte origin of podocysts, can be rejected because no amoebocytes are distributed throughout the mesoglea, which is much thinner than the cell size, throughout the podocyst production (Fig. 2, 3). Amoebocytes have not been discovered from the mesoglea in the polyps of *Aurelia* sp. in spite of carefully histochemical surveys (Yuan et al., 2008). The septal muscles, which extend from the oral disc to the bottom of calyx within the septa, sometimes give the misleading appearance of an intra-mesogleal component depending on the planes of histological sections but are not involved in podocyst production (Fig. 2A). Chapman (1970a) proposed that the podocyst production in *A. aurita* involves two processes: formation by pedal disc ectoderm alone, and the combination of the pedal

disc ectoderm and amoebocytes. However, it is unlikely that the developmentally identical structure is formed in distinct histological processes. No significant histological changes occur in the endoderm of polyps during podocyst production as has mentioned in previous studies, suggesting that endoderm is not directly involved in the podocyst production (D. M. Chapman, 1968, 1970a; Magnusen, 1980).

Formation of podocyst cells occur by the direct transformation of ectodermal cells, rather than by mediated stem cell formation, as has suggested by Chapman (1970a). No degradation of the pedal disc ectoderm occurs in the pedal-disc expanding stage (Fig. 3). Furthermore, the ectodermal cells along the invagination progressively transform into the podocyst cells with proceeding the podocyst production (Fig. 4, 5). In the polyps of *Aurelia*, epitheliomuscular cells can produce various types of cells through the unequal division producing amoebocytes like stem cells (Steinberg, 1963). However, the production of stem cells from the committed ectodermal cells was not observed throughout the podocyst production (Fig. 3B, 4B), and the transformation into podocyst cells do not therefore pass through the stem cell formation.

Transformation of the ectodermal cells considerably reverses the developmental process. The developmental stage of completed podocysts is equivalent to the blastula in the embryonic development, as both forms lack internal tissue differentiation and undergo ectoderm-endoderm differentiation (gastrulation) to become planula at the next stage (Thein et al., 2012; Yuan et al., 2008). The cell mass of podocysts can give rise to a whole polyp even after being divided into small pieces, suggesting that the podocyst cells are pluripotent (Black et al., 1976; Ikeda et al., 2011a). These features suggest that the transformation of the ectodermal cells during podocyst production can be classified as dedifferentiation, in which somatic cells revert to embryonic cells, rather than

transdifferentiation, in which one tissue directly transforms into the other tissue (Sugimoto et al., 2011). However, the dedifferentiation of podocyst cells should be verified by molecular analysis in future study.

Establishment of the oral-aboral axis in podocysts can be explained by the fact that the primary podocyst cells located at the bottom of the podocyst retain aborality and the podocyst cells moved to the top exert orality (Fig. 7A). This process does not disrupt the original oral-aboral relationship of the tissues in the parental polyps. If the podocysts were formed by randomly arranged cells, as in Chapman (1968), some external input of information would be required to produce the oral-aboral axis. During excystment, the formation of secretory granules containing enzymes that dissolve the podocyst capsule occurs in the apical cells of the podocyst, and the manubrium and tentacles form from the apical side even after 3 years of dormancy in *A. coerulea* and 6 years of dormancy in *Nemopilema nomurai* (Ikeda et al., 2011a; Thein et al., 2012), suggesting that the oral-aboral axis in podocysts is robustly maintained during elongated dormancy.

Development of associated structures

Podocyst capsule is formed by the transforming podocyst cells and the peripheral ectodermal cells, as these cells have secretory vesicles at the apical cytoplasmic region, proximal to the capsule formation (Fig. 3, 4). Particularly, in the invaginating ectoderm of the pedal disc, the cells on both sides secrete materials into the interspace to form the podocyst capsule (Fig. 3C), indicating that the capsule material is secreted internally by the podocyst cells and externally by the ectodermal cells. These results are consistent with the description of podocyst formation in *Cyanea lamarckii* by Widersten (1969). At

the end of podocyst formation, the podocyst cells have the vesicles, but the outer ectodermal cells do not, suggesting that the closure of the podocyst capsule is completed by the podocyst cells internally (Fig. 7C). These vesicles are identical to those of the secretory ectodermal cells in the stalk and pedal disc at the pre-production stage, showing dark red stain in the Fe-ECR test (Fig. 2, 3, 4). The secretory ectoderm on the lower body of polyps forms the pedal cuticle, which serves as an adhesive interface between a polyp and a substrate (Fig. 2B, see Chapman 1968). These facts suggest that the podocyst capsule and the pedal cuticle share the chemical materials, chitin-protein complex, as well as the secretory cells (Blanquet, 1972).

Accumulation of nutrient substances is the essential process for the podocysts to maintain prolonged dormancy (Black, 1981; Ikeda et al., 2011a; Thein et al., 2012). The nutrient granules containing polysaccharides and proteins are formed within the cytoplasm of the podocyst cells from the capsule-forming stage (Fig. 4). Additionally, no exogenous supply of nutrient granules from the peripheral tissues was observed throughout the capsule-forming stage (Fig. 4, 5). These facts suggest the endogenous synthesis of energy reserve substances by the podocyst cells. The quantity of the substances stored in podocyst cells is substantial, resulting in a significant increase in cell height from 10 μm (Fig. 2A) to 100 μm (Fig. 5A) as granule accumulation progresses. However, during the pedal-disc expansion stage, the pedal disc ectodermal cells have limited nutrient reserves, as evidenced by their weak histochemical responses to these substances (Fig. 3B, C). This observation suggests that the materials of nutrients for the podocyst cells must come from other surrounding tissues.

One potential source of the nutrient materials is the stalk ectoderm, which contains numerous protein vesicles (Fig. 2, 3). However, these vesicles are primarily

used for the formation of podocyst capsules (Fig. 4C) and are therefore unlikely to be converted to nutrient granules. In the freshwater hydra *Hydra vulgaris*, nutrient substances in the yolk of oocytes are provided through the phagocytosis of circumference nurse cells (Tardent, 1974; Technau et al., 2003). In the podocysts of *A. coerulea*, however, no morphological evidence of phagocytosis was observed in the ectodermal cells of the pedal disc during the podocyst production (Fig. 3, 4). Consequently, it is improbable that the pedal disc ectoderm plays a role in supplying the nutrient to the podocyst cells.

Another potential source of nutrients is the endoderm. The gastrovascular endodermal cells in the calyx of polyps store numerous protein and lipid granules in their cytoplasm (Fig. 2A, B). The endoderm is physically separated from the ectoderm with a thin mesogleal layer (ca. 2.5 μm in thickness) through the period of podocyst formation (Fig. 2, 4, 5). In *H. vulgaris*, trans-mesogleal cytoplasmic projection or direct cell penetration connects between ectoderm and endoderm (Sarras et al., 1993; Shimizu et al., 2008). Such structure cannot be observed in the pedal disc mesoglea of *A. coerulea* (Fig. 3B). This fact suggests that the direct transportation of nutrients from the endoderm to the ectoderm does not occur in the podocyst production. In Cnidaria, digested products absorbed by the endoderm reach the ectoderm by diffusing across the mesoglea (Chapman & Pardy, 1972). The vitellogenic oocytes of scyphozoan medusae obtain nutrients from the circumference mesoglea in the ovary (Eckelbarger & Larson, 1992, 1988; Ikeda et al., 2011b). Hence, it is probable that the same systems play a role of the nutrient transport from the endoderm to pedal disc ectodermal cells during podocyst formation. No accumulation of nutrient vesicles was observed in the aboral bulge endoderm, directory above the podocyst cells, throughout the podocyst formation,

whereas the gastrovascular endoderm, distant from the podocyst cells, accumulate lipids inside (Fig. 2E, 4A, 5A). It is likely that the role of aboral bulge endoderm is simply a pathway for nutrients, and the nutrients are once transported from the gastrovascular endoderm to the aboral bulge endoderm and then to podocyst cells via mesoglea, although the primary role of the aboral bulge endoderm is hydrostatic skeleton in the stalk and stolons (Chapman, 1970b; Gilchrist, 1937). However, the histological technique did not allow us to determine whether tissues provide the nutrients to the podocysts.

Extracellular matrix of the polyps dynamically changes during the podocyst production, as the endoderm changes their structure and position (Fig. 3, 4, 6). In particular, the mass of extracellular matrix develops synchronously with the arrangement of podocyst cells at the capsule-tanning stage (Fig. 7). Chapman (1970a) proposed that this structure arises from the pinching of the pedal disc mesoglea by the retracting podocyst cells as a central clear zone. If this were the case, the pedal disc mesoglea would bend downwards due to tensile force. It is likely that the retracting podocyst cells themselves forms this extracellular matrix, serving a scaffold for their movement.

Relationship to the other asexual reproduction modes and dormant forms in Scyphozoa

Podocysts serve as the reproductive modes and dormant forms in the Order Discomedusae, which was formerly separated into Semaeostomeae and Rhizistomeae, in the Class Scyphozoa (Arai, 2009; Helm, 2018). The Order Coronatae, a sibling order of Discomedusae in Scyphozoa, has no podocyst in their life cycle (Jarms, 2010). Histological characters of podocysts are almost identical among the species in

Discomedusae (Black, 1981; D. M. Chapman, 1968; Ikeda et al., 2011a; Thein et al., 2013). In addition, the evolutionary origin of podocysts can be traced back to the common ancestor of Discomedusae (Dawson & Hamner, 2009). These facts suggest that the forming process, including the origin of cells and podocyst capsule as described in this study, is common in Discomedusae.

The differences between podocysts and stoloniferous cysts in production process remain unclear, as no stolonocyst was formed by the polyps in this study (Fig. 1). Stoloniferous cysts represent a subform of podocysts, being formed at the tip of extended stolons, and are observed in scyphozoan species, such as *A. coerulea* and *Catostylus mosaicus* (Pitt, 2000; Thein et al., 2012). In this study, the extension of stolons from the calyx to the podocyst was observed only after the capsule-tanning stage (Fig. 1). However, not all cyst formation patterns may be consistent with our observations, although podocysts and stoloniferous cysts have the same histological structure (Thein et al., 2012). The production of stoloniferous cyst possibly depends on species and environmental conditions.

Podocyst production is distinguished by its exclusive ectodermal origin from the asexual reproduction of scyphozoan polyps (Fig 4, 5, see Thein et al. 2012). In addition to podocyst production, scyphozoan polyps exhibit various modes of asexual reproduction, all of which include endodermal tissues. Polyp budding from the calyx and stolons represents a widespread mode of asexual reproduction to replicate polyps in Scyphozoa, and is caused by evagination involving both the ectoderm and endoderm (Arai, 1997; Balcer & Black, 1991). Free swimming buds, analogous to planulae, are asexual propagules released from the calyx of polyps in species such as *A. aurita*, *Cassiopea* spp., *Cephea cephea*, *Cotylorhiza tuberculata* and *Sanderia malayensis*,

exhibiting the coordinated evagination of ectoderm and endoderm similar to polyp budding (Adler & Jarms, 2009; Hofmann & Honegger, 1990; Kikinger, 1992; Kikinger & Salvini-Plawen, 1995; Sugiura, 1966). The polyps of *Chrysaopa* sp. and *S. malayensis* detach their tentacles, consisted of ectoderm and endoderm, which then move and develop into polyps like free swimming buds (Adler & Jarms, 2009; D. M. Chapman, 1970b; Hérouard, 1913). Longitudinal fission is a relatively minor mode of asexual reproduction that directly divides a polyp into two individuals, conducted by the polyps of *Aurelia* spp., *Catostylus mosaics*, *Cyanea capillata*, *Phasellophora camtschatica* and *Sanderia malayensis* (Adler & Jarms, 2009). Additionally, the polyps of *A. aurita* and *S. malayensis* release free swimming buds that originate from the endoderm of the gastric cavity and the inside of the stolons, referred to as called internal-produced free swimming propagules (Adler & Jarms, 2009; Vagelli, 2007). These differences in the histological origin of podocyst from the other asexual reproduction suggest that the podocysts have evolved independently from the other asexual reproductive modes in Discomedusae.

As dormant forms, podocysts have both similarities and differences with the other dormant forms in Scyphozoa. Planulocysts are a dormant form that are encysted by the planulae in a chitinous capsule immediately after settling on substrates and are observed in *Cyanea* species (Dong et al., 2006; Holst & Jarms, 2007). The histological structure of planulocysts is closely similar to that of podocysts, consisting of an anaplastic cell mass and a chitinous capsule (Dong et al., 2006; Holst et al., 2024). Additionally, the planulocysts excyst to give rise to a polyp with the degradation of the upper capsule, mirroring the process in podocysts (Fu et al., 2019; Holst et al., 2024; Ikeda et al., 2011a). However, the developmental origin is completely different; planulocysts

undergo whole-body encystment, whereas podocysts undergo partial ectodermal transformation (D. M. Chapman, 1970a; Holst et al., 2024). It remains unclear whether the morphological similarities between podocysts and planulocysts are merely convergent for dormancy or genetically related. Another dormant form in Scyphozoa is contracted polyps, which are degenerated polyps retracted into their chitinous peridermal tubes, observed in coronate species such as *Nausithoe maculata* (formerly named *N. aurea*) and *Nausithoe racemosa* (formerly named *Stephanoscyphus racemosus*) (Silveira et al., 2002; Werner, 1970). This dormant form has chitinous outer coats of peridermal tubes to protect somatic tissues like podocysts, although the tissues have a diploblastic structure as the result of weak degeneration of whole polyps (Silveira et al., 2002). This morphological feature distinguishes contracted polyps from podocysts. Furthermore, unlike podocysts, planulocysts and contracted polyps have no role in asexual reproduction (Holst et al., 2024; Silveira et al., 2002). Therefore, podocysts appear to be evolutionarily and developmentally distinct from the other two dormant forms in Scyphozoa.

5. Conclusions

The current study has elucidated the histological process involved in the podocyst production in *Aurelia coerulea*. The exclusive ectodermal origin and direct dedifferentiation from somatic ectodermal cells distinguish the podocyst from the other modes of asexual reproduction and dormant forms, implying a unique evolutionary origin of the podocyst within the scyphozoan phylogeny. Throughout podocyst production, the ectodermal cells contribute to the formation of the podocyst cuticle and the extracellular matrix, and undergo the dynamic change in their own structures,

positions and differentiation state. These developmental characteristics probably reflect the high developmental plasticity of the ectodermal tissues in scyphozoan polyps.

Acknowledgements

We appreciate Ms. K. Koike of N-BARD at Hiroshima University for helping light microscopy. This work was financially supported by the research grant from the Fisheries Agency of Japan.

Literature cited

Adler, L., & Jarms, G. (2009). New insights into reproductive traits of scyphozoans: Special methods of propagation in *Sanderia malayensis* Goette, 1886 (Pelagiidae, Semaeostomeae) enable establishing a new classification of asexual reproduction in the class Scyphozoa. *Marine Biology*, *156*(7), 1411. https://doi.org/10.1007/s00227-009-1181-6

Arai, M. N. (1997). *A Functional Biology of Scyphozoa*. Springer Netherlands. https://doi.org/10.1007/978-94-009-1497-1

Arai, M. N. (2009). The potential importance of podocysts to the formation of scyphozoan blooms: A review. *Hydrobiologia*, *616*(1), 241–246. https://doi.org/10.1007/s10750-008-9588-5

Balcer, L. J., & Black, R. E. (1991). Budding and strobilation in *Aurelia* (Scyphozoa, Cnidaria): Functional requirement and spatial patterns of nucleic acid synthesis. *Roux's Archives of Developmental Biology*, *200*(1), 45–50. https://doi.org/10.1007/BF02457640

Black, R. E. (1981). Metabolism and ultrastructure of dormant podocysts of *Chrysaora quinquecirrha* (Scyphozoa). *Journal of Experimental Zoology Part A: Ecological Genetics and Physiology*, *218*(2), 175–182. https://doi.org/10.1002/jez.1402180210

Black, R. E., Enright, R. T., & Sung, L. (1976). Activation of the dormant podocyst of *Chrysaora quinquecirrha* (Schyphozoa) by removal of the cyst covering. *Journal of Experimental Zoology Part A: Ecological Genetics and Physiology*, *197*(3), 403–413. https://doi.org/10.1002/jez.1401970313

Blanquet, R. S. (1972). Structural and chemical aspects of the podocyst cuticle of the

scyphozoan medusa, *Chrysaora quinquecirrha*. *The Biological Bulletin*, *142*(1), 1–10. https://doi.org/10.2307/1540241

Calder, D. R. (1973). Laboratory observations on the life history of *Rhopilema verrilli* (Scyphozoa: Rhizostomeae). *Marine Biology*, *21*(2), 109–114. https://doi.org/10.1007/BF00354606

Cargo, D. G., & Rabenold, G. E. (1980). Observations on the asexual reproductive activities of the sessile stages of the sea nettle *Chrysaora quinquecirrha* (Scyphozoa). *Estuaries and Coasts*, *3*(1), 20–27. https://doi.org/10.2307/1351931

Chapman, D. M. (1968). Structure, histochemistry and formation of the podocyst and cuticle of *Aurelia aurita*. *Journal of the Marine Biological Association of the United Kingdom*, *48*(1), 187–208. https://doi.org/10.1017/S0025315400032537

Chapman, D. M. (1970a). Further observations on podocyst formation. *Journal of the Marine Biological Association of the United Kingdom*, *50*(1), 107–111. https://doi.org/10.1017/S0025315400000631

Chapman, D. M. (1970b). Reextension mechanism of a scyphistoma's tentacle. *Canadian Journal of Zoology*, *48*(5), 931–943. https://doi.org/10.1139/z70-168

Chapman, G., & Pardy, R. L. (1972). The movement of glucose and glycine through the tissues of *Corymorpha palma* Torrey (Coelenterata, Hydrozoa). *Journal of Experimental Biology*, *56*(3), 639–645.

Dawson, M. N., & Hamner, W. M. (2009). A character-based analysis of the evolution of jellyfish blooms: Adaptation and exaptation. *Hydrobiologia*, *616*(1), 193–215. https://doi.org/10.1007/s10750-008-9591-x

Dong, J., Liu, C., Wang, Y., & Wang, B. (2006). Laboratory observations on the life cycle of *Cyanea nozakii* (Semaeostomida, Scyphozoa). *Acta Zoologica Sinica*, *52*(2),

389–395.

Eckelbarger, K. J., & Larson, R. (1992). Ultrastructure of the ovary and oogenesis in the jellyfish *Linuche unguiculata* and *Stomolophus meleagris*, with a review of ovarian structure in the Scyphozoa. *Marine Biology*, *114*(4), 633–643.

Eckelbarger, K. J., & Larson, R. L. (1988). Ovarian morphology and oogenesis in *Aurelia aurita* (Scyphozoa: Semaeostomae): Ultrastructural evidence of heterosynthetic yolk formation in a primitive metazoan. *Marine Biology*, *100*(1), 103–115. https://doi.org/10.1007/BF00392960

Fu, Z., Xing, Y., Gu, Z., Liu, C., & Chen, S. (2019). Effects of temperature, salinity and dissolved oxygen on excystment of podocysts in the edible jellyfish *Rhopilema esculentum* Kishinouye, 189. *Indian Journal of Fishery*, *66*(4), 69–77.

Fuentes, V., Straehler-Pohl, I., Atienza, D., Franco, I., Tilves, U., Gentile, M., Acevedo, M., Olariaga, A., & Gili, J. (2011). Life cycle of the jellyfish *Rhizostoma pulmo* (Scyphozoa: Rhizostomeae) and its distribution, seasonality and inter-annual variability along the Catalan coast and the Mar Menor (Spain, NW Mediterranean). *Marine Biology*, *158*(10), 2247–2266. https://doi.org/10.1007/s00227-011-1730-7

Gilchrist, F. G. (1937). Budding and locomotion in the scyphistomas of *Aurelia*. *The Biological Bulletin*, *72*(1), 99–124.

Hadži, J. V. (1912). Über die Podozysten der Scyphopolypen. *Biologisches Zentralblatt*, *32*, 52–60.

Han, C., & Uye, S. (2010). Combined effects of food supply and temperature on asexual reproduction and somatic growth of polyps of the common jellyfish *Aurelia aurita* s.l. *Plankton and Benthos Research*, *5*(3), 98–105.

https://doi.org/10.3800/pbr.5.98

Heins, A., Glatzel, T., & Holst, S. (2015). Revised descriptions of the nematocysts and the asexual reproduction modes of the scyphozoan jellyfish *Cassiopea andromeda* (Forskål, 1775). *Zoomorphology*, *134*(3), 351–366. https://doi.org/10.1007/s00435-015-0263-x

Helm, R. R. (2018). Evolution and development of scyphozoan jellyfish. *Biological Reviews*, *93*(2), 1228–1250. https://doi.org/10.1111/brv.12393

Hérouard, E. (1912). Histoire du kyste pédieux de *Chrysaora* et sa signification. *Archives de Zoologie Expérimentale et Générale*, *5*(10), 11–25.

Hérouard, E. (1913). Relations entre la dépression et la formation de pseudoplanula tentaculaires chez le schyphistome. *Comptes rendus hebdomadaires des séances de l'Académie des sciences*, *156*, 1093–1095.

Hofmann, D. K., & Honegger, T. G. (1990). Bud formation and metamorphosis in *Cassiopea andromeda* (Cnidaria: Scyphozoa): A developmental and ultrastructural study. *Marine Biology*, *105*(3), 509–518. https://doi.org/10.1007/BF01316322

Holst, S., & Jarms, G. (2007). Substrate choice and settlement preferences of planula larvae of five Scyphozoa (Cnidaria) from German Bight, North Sea. *Marine Biology*, *151*(3), 863–871. https://doi.org/10.1007/s00227-006-0530-y

Holst, S., Kaiser, L., & Sötje, I. (2024). Planula settlement and polyp morphogenesis in two bloom forming jellyfish species of the genus *Cyanea* Péron and Lesueur, 1810 and effects of abiotic factors on planulocysts. *Marine Biology*, *171*(1), 6. https://doi.org/10.1007/s00227-023-04315-z

Hoover, R. A., & Purcell, J. E. (2009). Substrate preferences of scyphozoan *Aurelia*

labiata polyps among common dock-building materials. *Hydrobiologia*, *616*(1), 259–267. https://doi.org/10.1007/s10750-008-9595-6

Ikeda, H., Ohtsu, K., & Uye, S. (2011a). Fine structure, histochemistry, and morphogenesis during excystment of the podocysts of the giant jellyfish *Nemopilema nomurai* (Scyphozoa, Rhizostomeae). *The Biological Bulletin*, *221*(3), 248–260. https://doi.org/10.1086/BBLv221n3p248

Ikeda, H., Ohtsu, K., & Uye, S. (2011b). Structural changes of gonads during artificially induced gametogenesis and spawning in the giant jellyfish *Nemopilema nomurai* (Scyphozoa: Rhizostomeae). *Journal of the Marine Biological Association of the United Kingdom*, *91*(1), 215–227. https://doi.org/10.1017/S0025315410001244

Imai, Y., Sue, A., & Yamaguchi, A. (1968). A removing method of the resin from epoxy-embedded sections for light microscopy. *Journal of Electron Microscopy*, *17*(1), 84–85. https://doi.org/10.1093/oxfordjournals.jmicro.a049599

Jarms, G. (2010). The early life history of Scyphozoa with emphasis on Coronatae, a review with a list of described life cycles. *Verhandlungen Des Naturwissenschaftlichen Vereins in Hamburg*, *45*, 17–31.

Kawahara, M., Ohtsu, K., & Uye, S. (2013). Bloom or non-bloom in the giant jellyfish *Nemopilema nomurai* (Scyphozoa: Rhizostomeae): Roles of dormant podocysts. *Journal of Plankton Research*, *35*(1), 213–217. https://doi.org/10.1093/plankt/fbs074

Kikinger, R. (1992). *Cotylorhiza tuberculata* (Cnidaria: Scyphozoa)—Life History of a Stationary Population. *Marine Ecology*, *13*(4), 333–362. https://doi.org/10.1111/j.1439-0485.1992.tb00359.x

Kikinger, R., & Salvini-Plawen, L. (1995). Development from polyp to stauromedusa in

Stylocoronella (Cnidaria: Scyphozoa). *Journal of the Marine Biological Association of the United Kingdom*, *75*(4), 899–912. https://doi.org/10.1017/S0025315400038236

Lendenfeld, R. (1884). The scyphomedusae of the southern hemisphere. Part III. *Proceedings of the Linnean Society of New South Wales*, *9*, 259–306.

Lotan, A., Ben-Hillel, R., & Loya, Y. (1992). Life cycle of *Rhopilema nomadica*: A new immigrant scyphomedusan in the Mediterranean. *Marine Biology*, *112*(2), 237–242. https://doi.org/10.1007/BF00702467

Lucas, C. H., Graham, W. M., & Widmer, C. (2012). Jellyfish life histories: Role of polyps in forming and maintaining scyphomedusa populations. *Advances in Marine Biology*, *63*, 133–196. https://doi.org/10.1016/B978-0-12-394282-1.00003-X

Magnusen, J. E. (1980). Epidermal cell movement during podocyst formation in *Chrysaora quinquecirrha*. In P. Tardent & R. Tardent (Eds.), *Developmental and cellular biology of coelenterates: Proceedings of the 4th International Coelenterates Conference held in Interlaken, Switzerland, 4-8* (pp. 435–440). Elsevir/North-Holland Biomedical Press.

Mayorova, T. D., Kosevich, I. A., & Melekhova, O. P. (2012). On some features of embryonic development and metamorphosis of *Aurelia aurita* (Cnidaria, Scyphozoa). *Russian Journal of Developmental Biology*, *43*(5), 271–285. https://doi.org/10.1134/S1062360412050050

Pitt, K. A. (2000). Life history and settlement preferences of the edible jellyfish *Catostylus mosaicus* (Scyphozoa: Rhizostomeae). *Marine Biology*, *136*(2), 269–279. https://doi.org/10.1007/s002270050685

Rato, L. D., Pinto, C., Duarte, I. M., Leandro, S. M., & Marques, S. C. (2021). Euryhalinity and thermal tolerance of *Phyllorhiza punctata* (Scyphozoa) scyphostomae: Life history and physiological trade-offs. *Marine Biology*, *168*(11), 158. https://doi.org/10.1007/s00227-021-03969-x

Sarras, M. P., Zhang, X., Huff, J. K., Accavitti, M. A., St. John, P. L., & Abrahamson, D. R. (1993). Extracellular matrix (mesoglea) of *Hydra vulgaris*: III. Formation and function during morphogenesis of hydra cell aggregates. *Developmental Biology*, *157*(2), 383–398. https://doi.org/10.1006/dbio.1993.1143

Scorrano, S., Aglieri, G., Boero, F., Dawson, M. N., & Piraino, S. (2017). Unmasking *Aurelia* species in the Mediterranean Sea: An integrative morphometric and molecular approach. *Zoological Journal of the Linnean Society*, *180*(2), 243–267. https://doi.org/10.1111/zoj.12494

Shimizu, H., Aufschnaiter, R., Li, L., Sarras, M. P., Borza, D., Abrahamson, D. R., Sado, Y., & Zhang, X. (2008). The extracellular matrix of hydra is a porous sheet and contains type IV collagen. *Zoology*, *111*(5), 410–418. https://doi.org/10.1016/j.zool.2007.11.004

Silveira, F., Jarms, G., & Morandini, A. (2002). Experiments in nature and laboratory observations with *Nausithoe aurea* (Scyphozoa: Coronatae) support the concept of perennation by tissue saving and confirm dormancy. *Biota Neotropica*, *2*(2), 1–25. https://doi.org/10.1590/S1676-06032002000200009

Stefanović, D., Stefanović, M., & Lalošević, D. (2015). Use of eriochrome cyanine R in routine histology and histopathology: Is it time to say goodbye to hematoxylin? *Biotechnic & Histochemistry*, *90*(6), 461–469. https://doi.org/10.3109/10520295.2015.1057765

Steinberg, S. N. (1963). The regeneration of whole polyps from ectodermal fragments of scyphistoma larvae of *Aurelia aurita*. *The Biological Bulletin*, *124*(3), 337–343.

Sugimoto, K., Gordon, S. P., & Meyerowitz, E. M. (2011). Regeneration in plants and animals: Dedifferentiation, transdifferentiation, or just differentiation? *Trends in Cell Biology*, *21*(4), 212–218. https://doi.org/10.1016/j.tcb.2010.12.004

Sugiura, Y. (1966). On the life-history of rhizostome medusae IV, *Cephea cephea*. *Embryologia*, *9*(2), 105–122. https://doi.org/10.1111/j.1440-169X.1966.tb00219.x

Takao, M., Okawachi, H., & Uye, S. (2014). Natural predators of polyps of *Aurelia aurita* s.l. (Cnidaria: Scyphozoa: Semaeostomeae) and their predation rates. *Plankton and Benthos Research*, *9*(2), 105–113.

Tardent, P. (1974). Gametogenesis in the genus *Hydra*. *Integrative and Comparative Biology*, *14*(2), 447–456. https://doi.org/10.1093/icb/14.2.447

Technau, U., Miller, M. A., Bridge, D., & Steele, R. E. (2003). Arrested apoptosis of nurse cells during *Hydra* oogenesis and embryogenesis. *Developmental Biology*, *260*(1), 191–206. https://doi.org/10.1016/S0012-1606(03)00241-0

Thein, H., Ikeda, H., & Uye, S. (2012). The potential role of podocysts in perpetuation of the common jellyfish *Aurelia aurita s.l.* (Cnidaria: Scyphozoa) in anthropogenically perturbed coastal waters. *Hydrobiologia*, *690*(1), 157–167. https://doi.org/10.1007/s10750-012-1045-9

Thein, H., Ikeda, H., & Uye, S. (2013). Ecophysiological characteristics of podocysts in *Chrysaora pacifica* (Goette) and *Cyanea nozakii* Kishinouye (Cnidaria: Scyphozoa: Semaeostomeae): Effects of environmental factors on their production, dormancy and excystment. *Journal of Experimental Marine Biology*

and Ecology, *446*, 151–158. https://doi.org/10.1016/j.jembe.2013.05.013

Treible, L. M., & Condon, R. H. (2019). Temperature-driven asexual reproduction and strobilation in three scyphozoan jellyfish polyps. *Journal of Experimental Marine Biology and Ecology*, *520*, 151204. https://doi.org/10.1016/j.jembe.2019.151204

Vagelli, A. A. (2007). New observations on the asexual reproduction of *Aurelia aurita* (Cnidaria, Scyphozoa) with comments on its life cycle and adaptive significance. *Invertebrate Zoology*, *4*(2), 111–127.

Werner, B. (1970). Contribution to the evolution in the genus *Stephanoscyphus* (Scyphozoa Coronatae) and ecology and regeneration qualities of *Stephanoscyphus racemosus* Komai. *Publications of the Seto Marine Biological Laboratory*, *18*(1), 1–20.

Widersten, B. (1969). Development of the periderm and podocysts in *Cyanea palmstruchi* Swartz 1809. *Zoologiska Birdag Från Uppsala*, *38*, 51–60.

Widmer, C. L., Fox, C., & Brierley, A. (2016). Effects of temperature and salinity on four species of northeastern Atlantic scyphistomae (Cnidaria: Scyphozoa). *Marine Ecology Progress Series*, *559*, 73–88. https://doi.org/10.3354/meps11879

Yamaguchi, T., Yokokawa, M., Suzuki, M., Higashide, S., Katoh, Y., Sugiyama, S., & Misaki, T. (2000). The time course of elastin fiber degeneration in a rat aneurysm model. *Surgery Today*, *30*(8), 727–731. https://doi.org/10.1007/s005950070085

Yuan, D., Nakanishi, N., Jacobs, D. K., & Hartenstein, V. (2008). Embryonic development and metamorphosis of the scyphozoan *Aurelia*. *Development Genes and Evolution*, *218*(10), 525–539. https://doi.org/10.1007/s00427-008-0254-8

Figure Legends

Fig. 1: Sequence of the morphological changes underneath the polyps of *Aurelia coerulea* during the formation of podocysts. A. Pre-production stage. Arrowheads denote the edge of pedal disc (pe) with a basal cuticle. B. Pedal-disc expansion stage. Note the enlargement of the pedal disc area compared to A., C. Capsule-forming stage. A capsule (ca) of a new podocyst (pd) is formed. D. Capsule-tanning stage. t, tentacle.

Fig. 2. Histological structure of the polyps of *Aurelia coerulea* in the pre-production stage. A. A longitudinal section of a whole polyp stained with HEVB. B. A longitudinal section through the lateral half of a polyp stained with TB. A thin mesoglea (mes and arrowheads) separates the ectoderm (ect) and the scyphopharyngeral, tenticular and gastrovascular endoderm (enm, ent and eng, respectively) from the manubrium to the bottom of calyx. Granules stained in pale blue in the gastrovascular endoderm contain lipids. C. A magnified view of the pedal disc surrounded by a pedal cuticle (pec) stained with Fe-ECR. Note that the stalk ectoderm (ecs) includes many small vesicles stained in red. D. A magnified view of the manubrium and the bottom of tentacles stained with TB. Note that no cellular component is seen in the thickened mesoglea. ecp, pedal disc ectoderm; enb, aboral bulge endoderm; m, manubrium; nc, nematocyst; pe, pedal disc; r, rivet; spm, septal muscle; t, tentacle.

Fig. 3. Internal structure of the polyps of *Aurelia coerulea* in the pedal-disc expansion

stage. A. A longitudinal section stained with HEVB. Arrowheads denote the stalk ectoderm (ecs) newly involved to the pedal disc. B. A magnified view of the extended ectoderm at the peripheral pedal disc stained with Fe-ECR. Note that the pedal cuticle is diminished. end, endoderm; mes, mesoglea; spm, septal muscle; pe, pedal disc.

Fig. 4. Light microscopy of the polyps of *Aurelia coerulea* in the early capsule-forming stage. A. A longitudinal section of the pedal disc stained with Fe-ECR. Note that the cells of the primary podocyst (pd) keeps seamless connection to the ectoderm (ect), and the mesoglea (mes and arrowheads) keep separating the cells of primary podocyst from the aboral bulge endoderm (enb). B. Histochemical reaction of the podocyst cells for polysaccharides that are stained purple red with PAS method. C. A magnified view of the boundary between the podocyst and the ectoderm stained with Fe-ECR. The podocyst capsule (ca) is formed in the interspace of the invaginated ectoderm having red vesicles. Pec, pedal cuticle.

Fig. 5. Light microscopy of the polyps of *Aurelia coerulea* in the late capsule-forming stage. A. A longitudinal section of a growing podocyst (pd) associated with a formed capsule (ca) stained with HEVB. The podocyst cells are separated from the aboral bulge endoderm (enb) by a mesoglea (mes and arrowheads). B. Boundary between the podocyst cells and the ectoderm (ect) stained with Fe-ECR. C. Podocyst and ectodermal cells having polysaccharide granules stained in purple with PAS test. Note that the ectodermal cells inside the podocyst (asterisks) forms polysaccharide granules in the cytoplasm to transform into podocyst cells.

Fig. 6. Light microscopy of the polyps of *Aurelia acoerulea* in the capsule-tanning stage. A. Longitudinal section of podocysts (pd) in the early (right) and late (left) capsule-tanning stages stained with HEVB. Mesoglea (mes and arrowheads) B. A magnified view at the opeining of podocyst capsule (ca) in the early capsule-tanning stage stained with HEVB. Extracellular matrix (ecm) extends from the mesoglea into the podocyst cells (pc). C. Apical part of the late capsule-tanning stage of podocyst nearly closing its capsule stained with Fe-ECR. ect, ectoderm; end, endoderm.

Fig. 7. Histochemical reactions of the polyp and podocyst of *Aurelia coerulea* immediately after the completion of podocyst formation. A. A longitudinal section of a polyp and a podocyst stained with HEVB. Note the absence of extracellular matrix in the podocyst. B. A magnified view of a podocyst whose protein stained in red with Fe-ECR test in the podocyst. C. Polysaccharides stained in purple with PAS test. ca, capsule; ect, ectoderm; end, endoderm; m, manubrium; mes, mesoglea; pd, podocyst; pe, pedal disc; t, tentacle.

Fig. 8. Schematic diagram illustrating the histological changes o in the polyps of *Aurelia coerulea* during podocyst production. A. Pre-production stage: The pedal disc (pe) is small, primarily facilitating the attachment of the polyp to the substrate (sub) via the pedal cuticle (pec). B. Pedal disc expansion stage: The ectodermal cells (ect) along the stalk elongate to attach to the substrate and expand the pedal disc. C. Early capsule-forming stage: The pedal disc cells

transform into the podocyst cells (pd), which collaborate with the adjacent ectodermal cells to form the podocyst capsule (ca). D. Late capsule-forming stage: The capsule is elongated as the ectodermal invagination progresses, with internal cell transformation to the podocyst cells. E. Capsule-tanning stage: Podocyst cells are arranged radially with forming extracellular matrix (ecm) and closing the podocyst capsule. F. End of podocyst formation: The parental polyp detaches from the podocyst either by crawling the pedal disc or elongating the stalk. end, endoderm, mes, mesoglea.

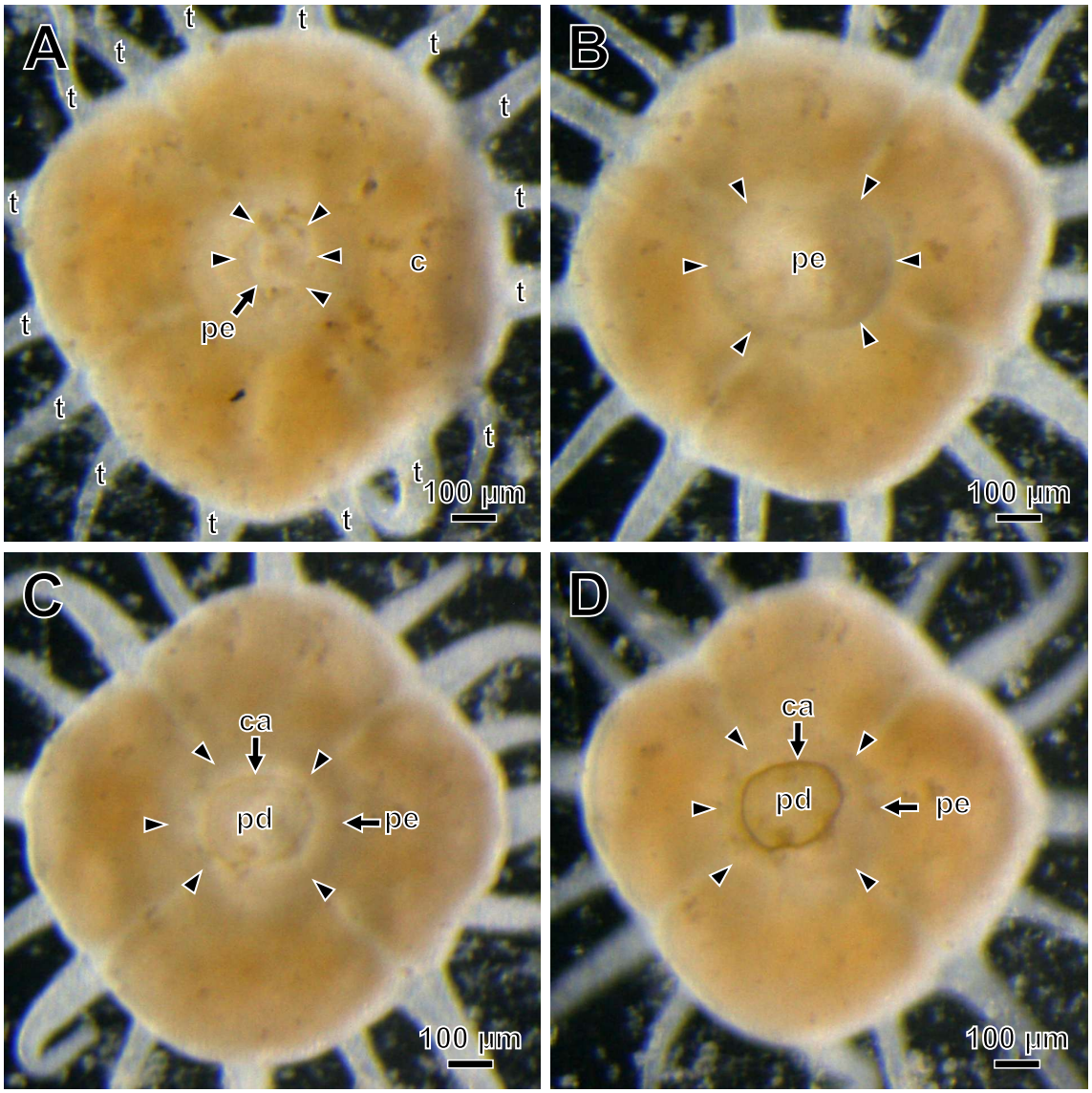

Fig. 1: Sequence of the morphological changes underneath the polyps of Aurelia coerulea during the formation of podocysts. A. Pre-production stage. Arrowheads denote the edge of pedal disc (pe) with a basal cuticle. B. Pedal-disc expansion stage. Note the enlargement of the pedal disc area compared to A., C. Capsule-forming stage. A capsule (ca) of a new podocyst (pd) is formed. D. Capsule-tanning stage. t, tentacle.

Figure 1

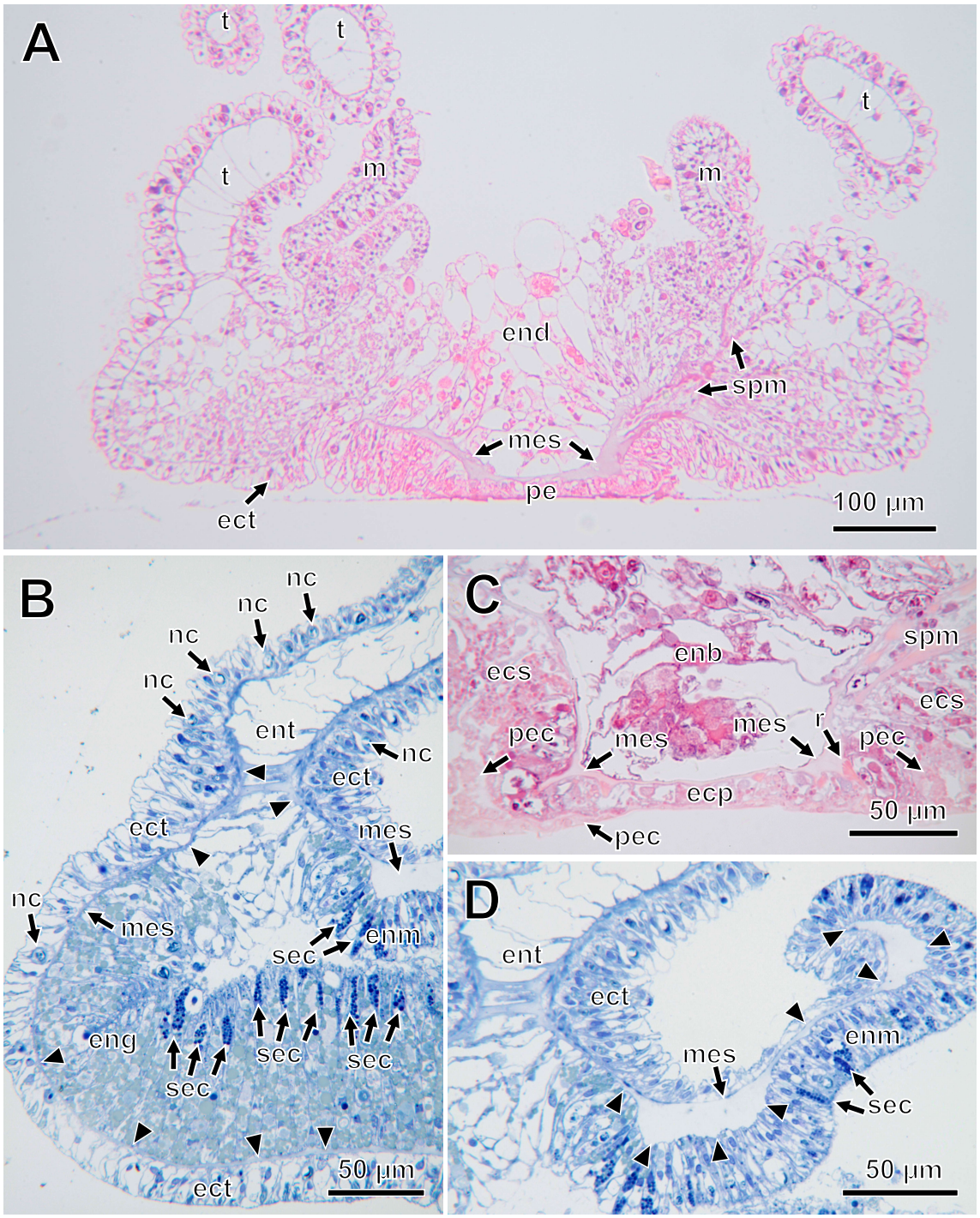

Fig. 2. Histological structure of the polyps of *Aurelia coerulea* in the pre-production stage. A. A longitudinal section of a whole polyp stained with HEVB. B. A longitudinal section through the lateral half of a polyp stained with TB. A thin mesoglea (mes and arrowheads) separates the ectoderm (ect) and the scyphopharyngeal, tenticular and gastrovascular endoderm (enm, ent and eng, respectively) from the manubrium to the bottom of calyx. Granules stained in pale blue in the gastrovascular endoderm contain lipids. C. A magnified view of the pedal disc surrounded by a pedal cuticle (pec) stained with Fe-ECR. Note that the stalk ectoderm (ecs) includes many small vesicles stained in red. D. A magnified view of the manubrium and the bottom of tentacles stained with TB. Note that no cellular component is seen in the thickened mesoglea. ecp, pedal disc ectoderm; enb, aboral bulge endoderm; m, manubrium; nc, nematocyst; pe, pedal disc; r, rivet; spm, septal muscle; t, tentacle.

Figure 2

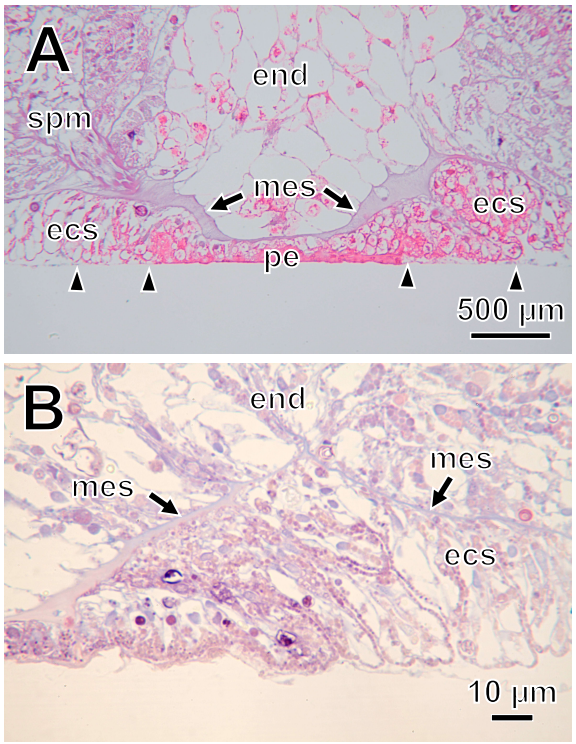

Fig. 3. Internal structure of the polyps of *Aurelia coerulea* in the pedal-disc expansion stage. A. A longitudinal section stained with HEVB. Arrowheads denote the stalk ectoderm (ecs) newly involved to the pedal disc. B. A magnified view of the extended ectoderm at the peripheral pedal disc stained with Fe-ECR. Note that the pedal cuticle is diminished. end, endoderm; mes, mesoglea; spm, septal muscle; pe, pedal disc.

Figure 3

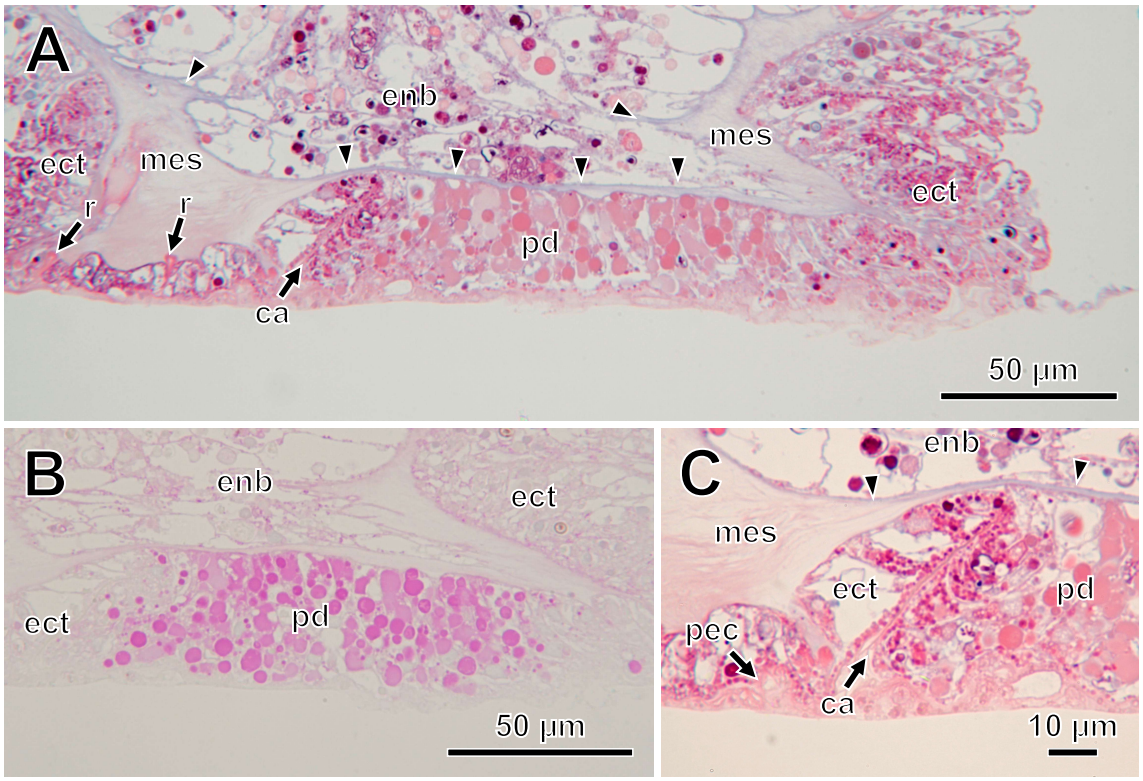

Fig. 4. Light microscopy of the polyps of *Aurelia coerulea* in the early capsule-forming stage. A. A longitudinal section of the pedal disc stained with Fe-ECR. Note that the cells of the primary podocyst (pd) keeps seamless connection to the ectoderm (ect), and the mesoglea (mes and arrowheads) keep separating the cells of primary podocyst from the aboral bulge endoderm (enb). B. Histochemical reaction of the podocyst cells for polysaccharides that are stained purple red with PAS method. C. A magnified view of the boundary between the podocyst and the ectoderm stained with Fe-ECR. The podocyst capsule (ca) is formed in the interspace of the invaginated ectoderm having red vesicles. Pec, pedal cuticle.

Figure 4

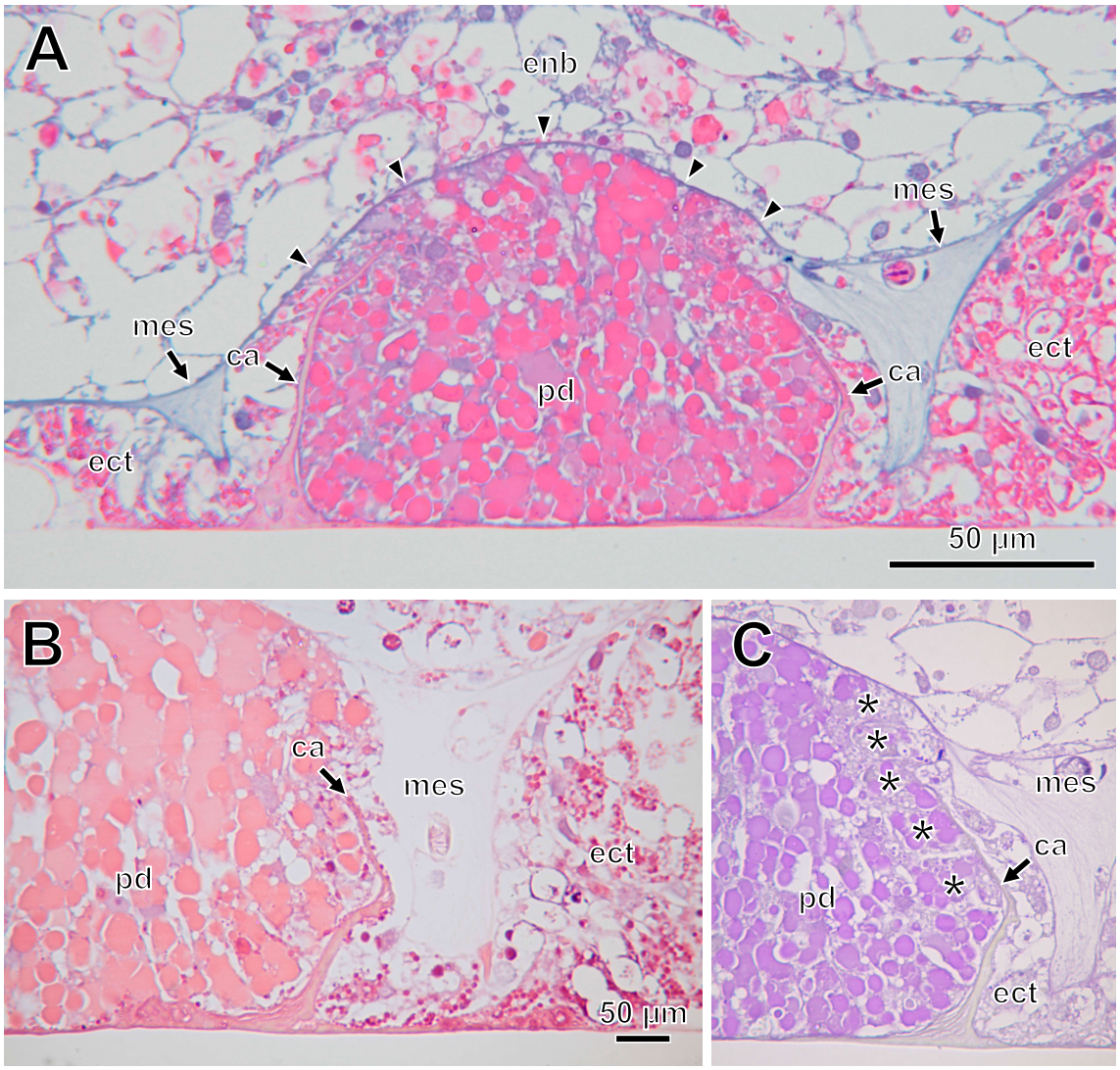

Fig. 5. Light microscopy of the polyps of Aurelia coerulea in the late capsule-forming stage. A. A longitudinal section of a growing podocyst (pd) associated with a formed capsule (ca) stained with HEVB. The podocyst cells are separated from the aboral bulge endoderm (enb) by a mesoglea (mes and arrowheads). B. Boundary between the podocyst cells and the ectoderm (ect) stained with Fe-ECR. C. Podocyst and ectodermal cells having polysaccharide granules stained in purple with PAS test. Note that the ectodermal cells inside the podocyst (asterisks) form polysaccharide granules in their cytoplasm and transform into podocyst cells..

Figure 5

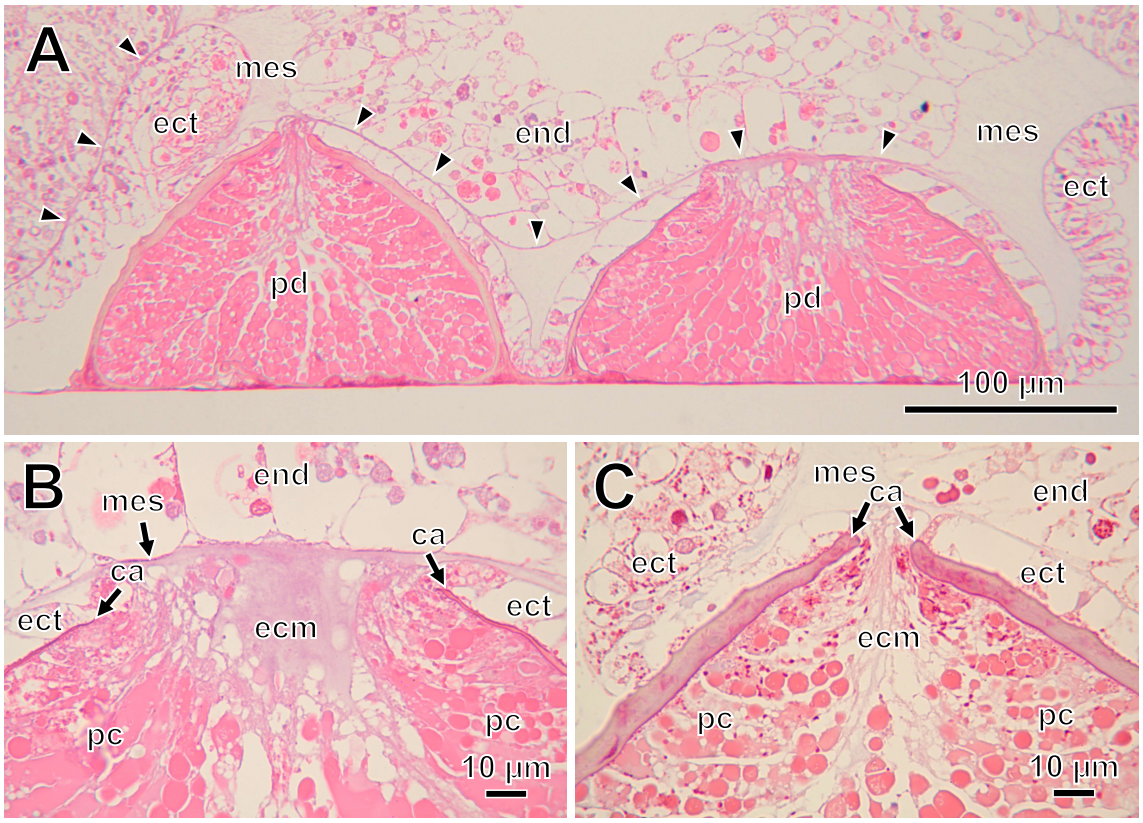

Fig. 6. Light microscopy of the polyps of *Aurelia acoerulea* in the capsule-tanning stage. A. Longitudinal section of podocysts (pd) in the early (right) and late (left) capsule-tanning stages stained with HEVB. Mesoglea (mes and arrowheads) B. A magnified view at the opeining of podocyst capsule (ca) in the early capsule-tanning stage stained with HEVB. Extracellular matrix (ecm) extends from the mesoglea into the podocyst cells (pc). C. Apical part of the late capsule-tanning stage of podocyst nearly closing its capsule stained with Fe-ECR. ect, ectoderm; end, endoderm.

Figure 6

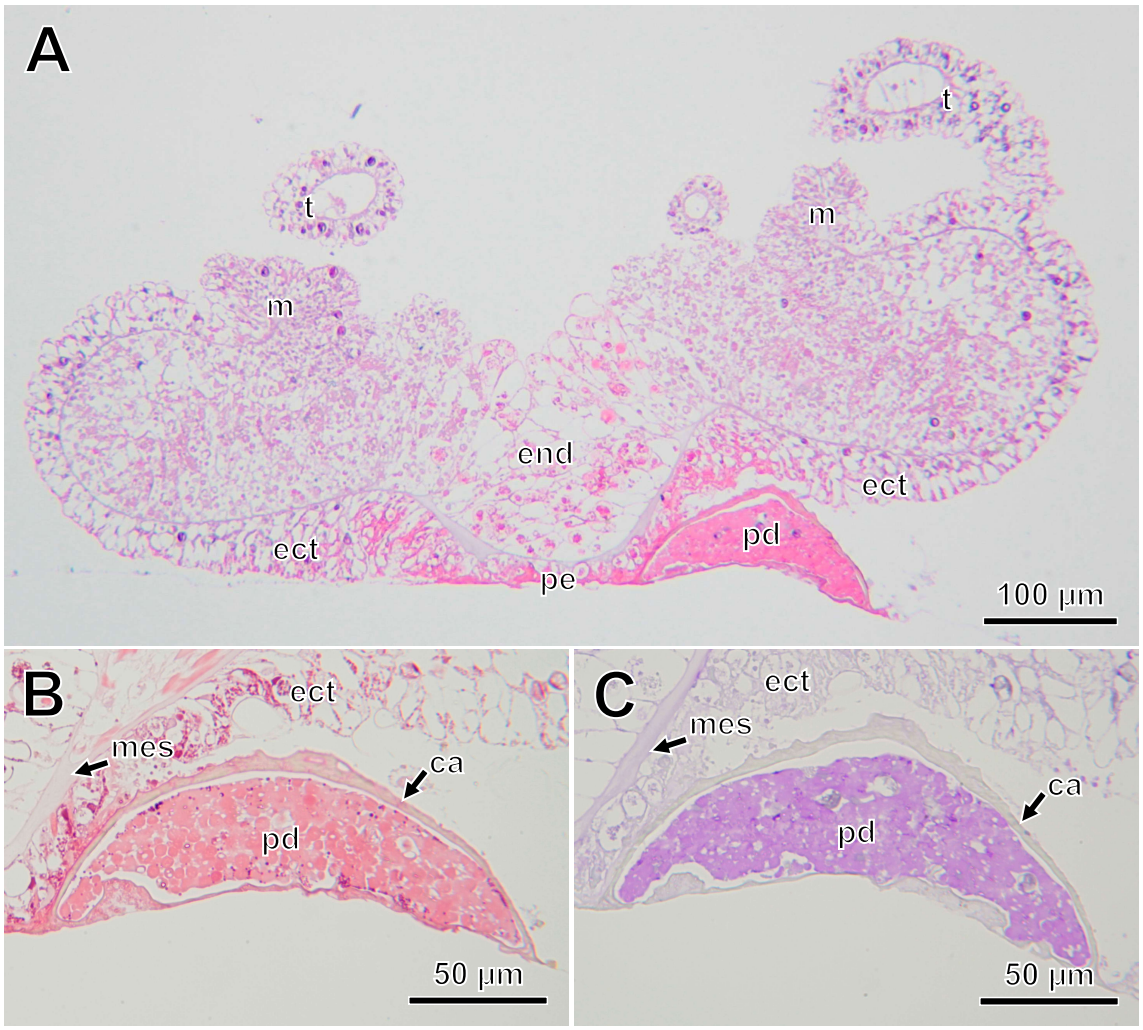

Fig. 7. Histochemical reactions of the polyp and podocyst of *Aurelia coerulea* immediately after the completion of podocyst formation. A. A longitudinal section of a polyp and a podocyst stained with HEVB. Note the absence of extracellular matrix in the podocyst. B. A magnified view of a podocyst whose protein stained in red with Fe-ECR test in the podocyst. C. Polysaccharides stained in purple with PAS test. ca, capsule; ect, ectoderm; end, endoderm; m, manubrium; mes, mesoglea; pd, podocyst; pe, pedal disc; t, tentacle.

Figure 7

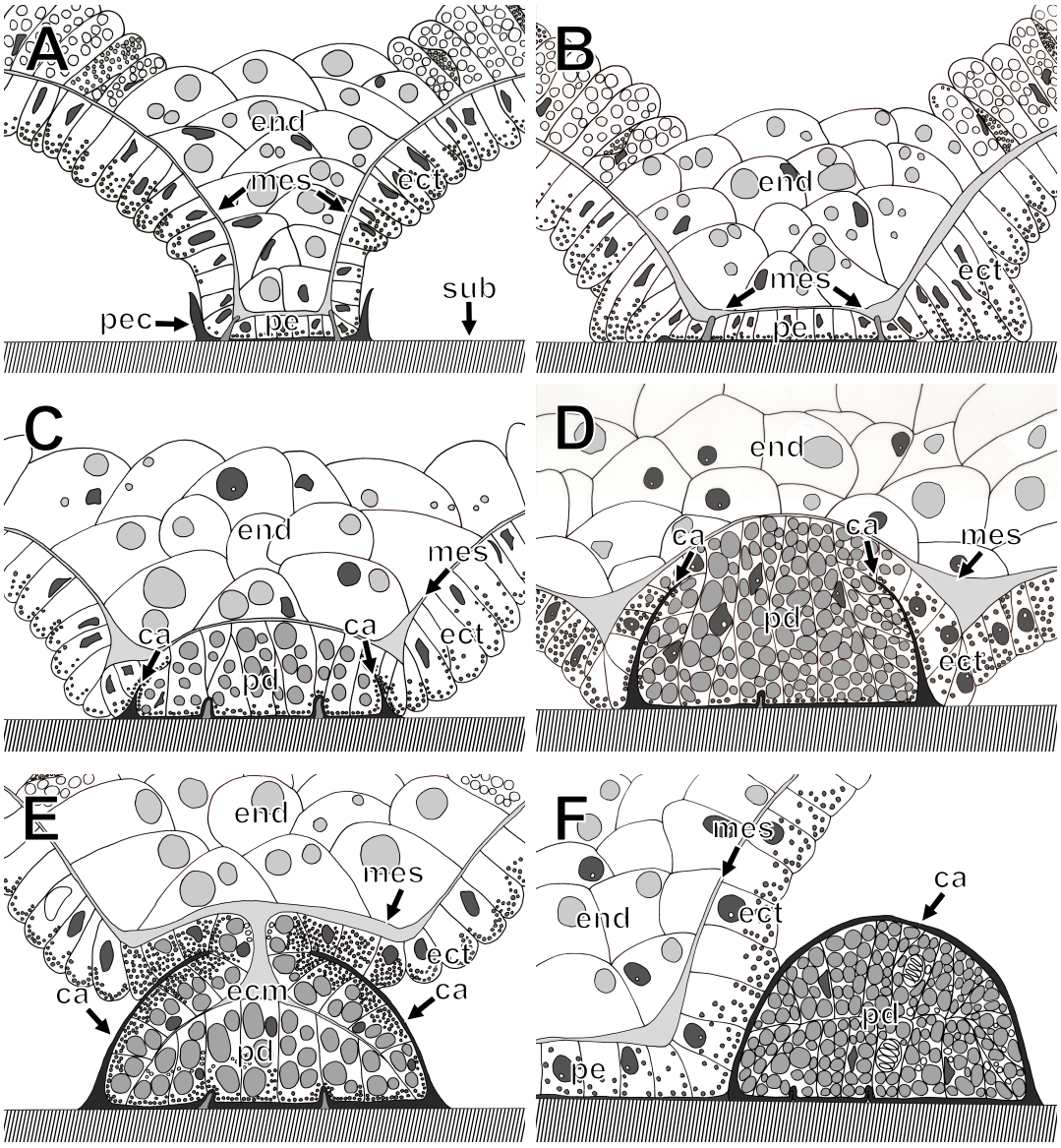

Fig. 8. Schematic diagram illustrating the histological changes o in the polyps of *Aurelia coerulea* during podocyst production. A. Pre-production stage: The pedal disc (pe) is small, primarily facilitating the attachment of the polyp to the substrate (sub) via the pedal cuticle (pec). B. Pedal disc expansion stage: The ectodermal cells (ect) along the stalk elongate to attach to the substrate and expand the pedal disc. C. Early capsule-forming stage: The pedal disc cells transform into the podocyst cells (pd), which collaborate with the adjacent ectodermal cells to form the podocyst capsule (ca). D. Late capsule-forming stage: The capsule is elongated as the ectodermal invagination progresses, with internal cell transformation to the podocyst cells. E. Capsule-tanning stage: Podocyst cells are arranged radially with forming extracellular matrix (ecm) and closing the podocyst capsule. F. End of podocyst formation: The parental polyp detaches from the podocyst either by crawling the pedal disc or elongating the stalk. end, endoderm, mes, mesoglea.

Figure 8

Appendix 1. List of the species of Discomedusae whose life cycle, asexual reproduction and the possession of dormant stages have been revealed. NS: not specified.

Taxon	Mode of asexual reproduction	Dormant stage	Reference
Cassiopea andromeda	External free swimming bud	NS	Hofmann et al. (1978)
Cassiopea xamachana	External free swimming bud	NS	Bigelow (1900)
Acromitus hardenbergi	Budding	NS	Miyake et al. (2021)
Aurelia aurita	Polyp budding, external free swimming bud, Internal free swimming bud, podocyst	Podocyst	Vagelli (2007), Sokołowski et al. (2916)
Aurelia coerulea	Polyp budding, external free swimming bud, fission, podocyst	Podocyst	Kakinuma (1975), Wang et al. (2023)
Aurelia labiata	Polyp budding, podocyst	Podocyst	Gershwin (2001)
Aurelia limbata	Polyp budding	NS	Uchida & Nagao (1963)
Aurelia relicta	Swimming bud, podocyst	Podocyst	Hubot et al. (2017)
Aurelia solida	Polyp budding, external free swimming bud, podocyst	Podocyst	Wang et al. (2023)
Catostylus mosaicus	Polyp budding, fission, podocyst	Podocyst	Pitt (2000)
Catostylus tagi	Podocyst	Podocyst	Gueroun et al. (2021)
Cephea cephea	External free swimming bud	NS	Sugiura (1966)
Chrysaora achlyos	Podocyst	Podocyst	Schaadt et al. (2001)
Chrysaora chesapeakei	Polyp budding, podocyst	Podocyst	Littleford (1939)
Chrysaora colorata	Podocyst	Podocyst	Gershwin & Collins (2002)
Chrysaora fuscescens	Podocyst	Podocyst	Widmer (2008)
Chrysaora hysoscella	Podocyst	Podocyst	Widmer et al. (2016)
Chrysaora lactea	Podocyst	Podocyst	Morandini et al. (2004)
Chrysaora pacifica	Podocyst	Podocyst	Kakinuma (1967)
Cotylorhiza tuberculata	External free swimming bud	NS	Kikinger (1992)
Cyanea capillata	Podocyst	Podocyst	Widmer et al. (2016)
Cyanea lamarckii	Polyp budding, podocyst	Podocyst, planulocyst	Widmer et al. (2016)
Cyanea nozakii	Podocyst	Podocyst	Dong et al. (2006)
Cyanea sp.	Podocyst	Podocyst, planulocyst	Brewer & Feingold (1991)
Lychnoriza lucerna	Podocyst	Podocyst	Schiariti et al. (2008)
Mastigias papua	External free swimming bud	NS	Sugiura (1963)
Nemopilema nomurai	Podocyst	Podocyst	Kawahara et al. (2006)
Pelagia noctiluca	NS	NS	Sandrini and Avian (1983)
Phacellophora camtschatica	Polyp budding, fission	NS	Widmer (2006)
Phyllorhiza punctata	External free swimming bud	NS	Rippingale & Kelly (1995)
Rhizostoma luteum	Podocyst	Podocyst	Kienberger et al. (2018)
Rhizostoma octopus	Polyp budding, podocyst	Podocyst	Holst et al. (2007)
Rhizostoma pulmo	Polyp budding, podocyst	Podocyst	Fuentes et al. (2011)
Rhopilema esculentum	Podocyst	Podocyst	You et al. (2007)
Rhopilema nomadica	Polyp budding, podocyst	Podocyst	Lotan et al. (1992)
Rhopilema verrilli	Podocyst	Podocyst	Calder (1973)
Sanderia malayensis	olyp budding, external free swimming bud, tentacle laceration, fission, gastric constrictio	NS	Adler & Jarms (2009)
Stomolophus meleagris	Polyp buddding, external free swimming bud, Podocyst	Podocyst	López-Martínez et al. (2023)

Appendix 2. List of the references cited in Appendix 1.

Adler, L., & Jarms, G. (2009). New insights into reproductive traits of scyphozoans: Special methods of propagation in *Sanderia malayensis* Goette, 1886 (Pelagiidae, Semaeostomeae) enable establishing a new classification of asexual reproduction in the class Scyphozoa. *Marine Biology*, *156*(7), 1411. doi: 10.1007/s00227-009-1181-6

Brewer, R. H., & Feingold, J. S. (1991). The effect of temperature on the benthic stages of *Cyanea* (Cnidaria: Scyphozoa), and their seasonal distribution in the Niantic River estuary, Connecticut. *Journal of Experimental Marine Biology and Ecology*, *152*(1), 49–60. doi: 10.1016/0022-0981(91)90134-I

Calder, D. R. (1973). Laboratory observations on the life history of *Rhopilema verrilli* (Scyphozoa: Rhizostomeae). *Marine Biology*, *21*(2), 109–114. doi: 10.1007/BF00354606

Dong, J., Liu, C., Wang, Y., & Wang, B. (2006). Laboratory observations on the life cycle of *Cyanea nozakii* (Semaeostomida, Scyphozoa). *Acta Zoologica Sinica*, *52*(2), 389–395.

Fuentes, V., Straehler-Pohl, I., Atienza, D., Franco, I., Tilves, U., Gentile, M., … Gili, J. (2011). Life cycle of the jellyfish *Rhizostoma pulmo* (Scyphozoa: Rhizostomeae) and its distribution, seasonality and inter-annual variability along the Catalan coast and the Mar Menor (Spain, NW Mediterranean). *Marine Biology*, *158*(10), 2247–2266. doi: 10.1007/s00227-011-1730-7

Gershwin, L. (2001). Systematics and biogeography of the jellyfish *Aurelia labiata* (Cnidaria: Scyphozoa). *The Biological Bulletin*, *201*(1), 104–119. doi: 10.2307/1543531

Gershwin, L., & Collins, A. G. (2002). A preliminary phylogeny of Pelagiidae (Cnidaria, Scyphozoa), with new observations of *Chrysaora colorata* comb. Nov. *Journal of Natural History*, *36*(2), 127–148. doi: 10.1080/00222930010003819

Gueroun, S. K. M., Torres, T. M., Dos Santos, A., Vasco-Rodrigues, N., Canning-Clode, J., &

Andrade, C. (2021). *Catostylus tagi* (Class: Scyphozoa, Order: Discomedusae, Suborder: Rhizostomida, Family: Catostylidae) life cycle and first insight into its ecology. *PeerJ*, *9*, e12056. doi: 10.7717/peerj.12056

Hofmann, D., Neumann, R., & Henne, K. (1978). Strobilation, budding and initiation of scyphistoma morphogenesis in the rhizostome *Cassiopea andromeda* (Cnidaria: Scyphozoa). *Marine Biology*, *47*, 161–176. doi: 10.1007/BF00395637

Holst, S., Sötje, I., Tiemann, H., & Jarms, G. (2007). Life cycle of the rhizostome jellyfish *Rhizostoma octopus* (L.) (Scyphozoa, Rhizostomeae), with studies on cnidocysts and statoliths. *Marine Biology*, *151*(5), 1695–1710. doi: 10.1007/s00227-006-0594-8

Hubot, N., Lucas, C. H., & Piraino, S. (2017). Environmental control of asexual reproduction and somatic growth of *Aurelia* spp. (Cnidaria, Scyphozoa) polyps from the Adriatic Sea. *PLOS ONE*, *12*(6), e0178482. doi: 10.1371/journal.pone.0178482

Kakinuma, Y. (1967). Development of a scyphozoan *Dactylometra pacifica* Goette. *Bulletin of the Marine Biological Station of Asamushi*, *13*(1), 29–33.

Kakinuma, Y. (1975). An experimental study of the life cycle and organ differentiation of *Aurelia aurita* Lamarck. *Bulletin of the Marine Biological Station of Asamushi*, *15*(3), 101–113.

Kawahara, M., Uye, S., Ohtsu, K., & Iizumi, H. (2006). Unusual population explosion of the giant jellyfish *Nemopilema nomurai* (Scyphozoa: Rhizostomeae) in East Asian waters. *Marine Ecology Progress Series*, *307*, 161–173.

Kienberger, K., Riera-Buch, M., Schönemann, A. M., Bartsch, V., Halbauer, R., & Prieto, L. (2018). First description of the life cycle of the jellyfish *Rhizostoma luteum* (Scyphozoa: Rhizostomeae). *PLOS ONE*, *13*(8), e0202093. doi: 10.1371/journal.pone.0202093

Kikinger, R. (1992). *Cotylorhiza tuberculata* (Cnidaria: Scyphozoa)—Life History of a

Stationary Population. *Marine Ecology*, *13*(4), 333–362. doi: 10.1111/j.1439-0485.1992.tb00359.x

Littleford, R. A. (1939). The life cycle of *Dactylometra quinquecirrha*, L. Agassiz in the Chesapeake Bay. *The Biological Bulletin*, *77*(3), 368–381. doi: 10.2307/1537646

López-Martínez, J., Álvarez-Tello, F. J., Porchas-Cornejo, M. A., Nevárez-López, C. A., Muhlia-Almazán, A., & Urías-Padilla, K. V. (2023). Multiple reproduction forms in the polyps of the cannonball jellyfish *Stomolophus* sp. 2: Probable life-cycle reversal. *Journal of Experimental Zoology Part A: Ecological and Integrative Physiology*, *339*(3), 239–252. doi: 10.1002/jez.2673

Lotan, A., Ben-Hillel, R., & Loya, Y. (1992). Life cycle of *Rhopilema nomadica*: A new immigrant scyphomedusan in the Mediterranean. *Marine Biology*, *112*(2), 237–242. doi: 10.1007/BF00702467

Miyake, H., Honda, S., Nishikawa, J., & Yusoff, F. M. (2021). Life cycle of edible jellyfish *Acromitus hardenbergi* Stiasny, 1934 (Scyphozoa: Rhizostomeae) inhabiting a brackish-water environment. *Animals*, *11*(7), 2138. doi: 10.3390/ani11072138

Morandini, A., da Silveira, F., & Jarms, G. (2004). The life cycle of *Chrysaora lactea* Eschscholtz, 1829 (Cnidaria, Scyphozoa) with notes on the scyphistoma stage of three other species. *Hydrobiologia*, *530–531*(1–3), 347–354. doi: 10.1007/s10750-004-2694-0

Pitt, K. A. (2000). Life history and settlement preferences of the edible jellyfish *Catostylus mosaicus* (Scyphozoa: Rhizostomeae). *Marine Biology*, *136*(2), 269–279. doi: 10.1007/s002270050685

Rippingale, R. J., & Kelly, S. J. (1995). Reproduction and survival of *Phyllorhiza punctata* (Cnidaria: Rhizostomeae) in a seasonally fluctuating salinity regime in Western Australia. *Marine and Freshwater Research*, *46*(8), 1145–1151. doi:

10.1071/mf9951145

Sandrini, L. R., & Avian, M. (1983). Biological cycle of *Pelagia noctiluca*: Morphological aspects of the development from planula to ephyra. *Marine Biology*, *74*(2), 169–174. doi: 10.1007/BF00413920

Schaadt, M., Yasukochi, L., Gershwin, L.-A., & Wrobel, D. (2001). Husbandry of the black jelly (*Chrysaora achlyos*), a newly discovered scyphozoan in the eastern North Pacific Ocean. *Bulletin de l'Institut Océanographique Monaco*, *20*, 289–296.

Schiariti, A., Kawahara, M., Uye, S., & Mianzan, H. W. (2008). Life cycle of the jellyfish *Lychnorhiza lucerna* (Scyphozoa: Rhizostomeae). *Marine Biology*, *156*(1), 1–12. doi: 10.1007/s00227-008-1050-8

Sokołowski, A., Brulińska, D., Olenycz, M., & Wołowicz, M. (2016). Does temperature and salinity limit asexual reproduction of *Aurelia aurita* polyps (Cnidaria: Scyphozoa) in the Gulf of Gdańsk (southern Baltic Sea)? An experimental study. *Hydrobiologia*, *773*(1), 49–62. doi: 10.1007/s10750-016-2678-x

Sommer, F. A. (1988). Developmental cycle of *Pelagia colorata*. *American Zoologist*, *28*(4), 170A.

Sugiura, Y. (1963). On the life-history of rhizostome medusa I. *Mastigias papua* L. Agassiz. *Annotationes Zoologicae Japonenses*, *36*(4), 194–202.

Sugiura, Y. (1966). On the life-history of rhizostome medusae IV, *Cephea cephea*. *Embryologia*, *9*(2), 105–122. doi: 10.1111/j.1440-169X.1966.tb00219.x

Uchida, T., & Nagao, Z. (1963). The metamorphosis of the scyphomedusa, *Aurelia limbata* (Brandt). *Annotationes Zoologicae Japonenses*, *36*(2), 83–91.

Vagelli, A. A. (2007). New observations on the asexual reproduction of *Aurelia aurita* (Cnidaria, Scyphozoa) with comments on its life cycle and adaptive significance. *Invertebrate Zoology*, *4*(2), 111–127.

Wang, F., Schiariti, A., Xu, S., Ma, Y., Wang, L., Zhao, J., & Dong, Z. (2023). Asexual reproduction strategies in the moon jellyfish *Aurelia* (Cnidaria: Scyphozoa). *Frontiers in Ecology and Evolution*, *10*. Retrieved from https://www.frontiersin.org/articles/10.3389/fevo.2022.1071518

Widmer, C. L. (2006). Life cycle of *Phacellophora camtschatica* (Cnidaria: Scyphozoa). *Invertebrate Biology*, *125*(2), 83–90. doi: 10.1111/j.1744-7410.2006.00043.x

Widmer, C. L. (2008). Life cycle of *Chrysaora fuscescens* (Cnidaria: Scyphozoa) and a Key to Sympatric Ephyrae1. *Pacific Science*, *68*(2), 71–82. doi: 10.2984/1534-6188(2008)62[71:LCOCFC]2.0.CO;2

Widmer, C. L., Fox, C., & Brierley, A. (2016). Effects of temperature and salinity on four species of northeastern Atlantic scyphistomae (Cnidaria: Scyphozoa). *Marine Ecology Progress Series*, *559*, 73–88. doi: 10.3354/meps11879

You, K., Ma, C., Gao, H., Li, F., Zhang, M., Qiu, Y., & Wang, B. (2007). Research on the jellyfish (*Rhopilema esculentum* Kishinouye) and associated aquaculture techniques in China: Current status. *Aquaculture International*, *15*(6), 479–488. doi: 10.1007/s10499-007-9114-1

Appendix 3. Raw data on parameters obtained for the study of the process of podocyst production.

Parameter	Calyx diameter of polyps	Number of formed podocysts per polyp	Size of pedal disc of polyps at pre-production stage	ımeter of pedal disc of polyps at pedal-disc expamsion st	Long base axis of newly formed podocysts	Base area of newly formed podocysts	Size of pedal disc at capsule-forming stage	Ratio of the size of podocyst to the pedal disc
Unit	μm	podocysts polyp^{-1}	μm	μm	μm	μm^2	μm^2	
1	1522.942	0	368.117	768.553	317.852	70276.717	356487.03	0.197136813
2	1261.947	1	317.116	573.789	350.469	70792.736	190547.773	0.371522243
3	1079.298	1	328.599	496.402	213.97	30013.706	106529.51	0.281740768
4	762.465	3	248.393	531.297	254.758	40405.744	131663.427	0.306886619
5	1542.36	1	598.156	710.166	240.556	40760.227	310690.687	0.131192304
6	1095.158	1	296.773	589.779	381.941	76268.236	143701.402	0.530741071
7	1215.342	0	235.128	686.437	244.01	34749.98	347670.94	0.099950775
8	797.392	3	204.972	632.359	303.739	61274.992	128298.054	0.477598764
9	819.814	3	365.422	718.549	248.547	37371.107	162493.333	0.229985479
10	1239.174	0	573.594	892.334	303.69	54993.315	268343.449	0.204936305
11	940.827	3	204.724	510.224	207.029	28387.11	124781.82	0.227493957
12	1052.875	1	223.132	893.032	254.025	44165.678	133123.689	0.331764229
13	929.636	0	414.672	609.53	223.608	34658.408	145039.387	0.238958594
14	1171.973	2	307.944	493.817	293.69	45712.975	203427.092	0.224714292
15	1200.498	1	244.649	875.46	267.363	47421.828	280075.792	0.16931784
16	1158.284	0	484.744	633.976	347.98	66389.02	245794.419	0.270099786
17	1105.616	0	408.138	636.119	381.602	97098.173	283144.014	0.342928574
18				521.598	248.615	43339.842	202477.662	0.214047523
19				768.265	321.646	57672.96	296815.397	0.194305823
20				687.222	286.706	52962.065	235558.663	0.224835989
Number of data	17	17	17	20	20	20	20	20
Max	1542.36	3	598.156	893.032	381.941	97098.173	356487.03	0.530741071
min	762.465	0	204.724	493.817	207.029	28387.11	106529.51	0.099950775
Average	1111.505941	1.176470588	342.6042941	661.4454	284.5898	51735.74095	214833.177	0.263507887
SD	222.3396414	1.185078801	121.4299285	128.761203	53.09714631	17703.14164	79887.98122	0.106712785

Appendix 4. Raw data of the parameters obtained for the histological measurements.

Parameter	Height of cells from the manubrium to to lateral calyxat at pre-production stage	Height of cells from the bottom of calyx to the stalk at pre-production stage	Thickness of mesoglea in the stalk of polyps at pedal-disc expansion stage	Thickness of mesoglea in the calyx of polyps at pedal-disc expansion stage	Diameter of granules in podocysts	Diameter of secretory vesicles
Unit	µm	µm	µm	µm	µm	µm
1	20,117	38,35	5,848	1,017	1,805	0,911
2	17,597	39,176	1,649	2,167	2,971	0,857
3	9,237	45,872	11,372	0,845	3,672	0,713
4	7,485	53,881	0,618	1,723	2,17	0,613
5	19,431	27,605	7,549	1,961	2,61	0,655
6	21,647	49,108	9,599	0,956	2,738	0,66
7	17,393	20,173	10,806	2,754	2,539	0,857
8	15,836	39,754	2,752	1,412	2,974	0,59
9	32,573		7,154	3,457	2,853	0,473
10	34,415		3,648	4,178	3,457	0,579
11	28,094		5,774	0,709	3,992	0,65
12	12,306		7,562	0,37	4,896	0,566
13			14,082	0,694	4,407	0,614
14			11,112	2,021	3,902	0,706
15			3,263	0,51	4,082	0,69
16			11,447	0,516	2,829	0,717
17			4,215	0,327	4,139	0,621
18			6,693	0,533	2,775	0,857
19			21,561	2,422	2,707	0,808
20			15,881	2,334	2,533	0,766
21			14,99	1,242	3,758	0,821
22			6,699	5,162	3,68	0,702
23			8,384	1,686	2,864	0,722
24			16,465	0,998	4,092	0,789
25			6,553	0,482	3,792	0,909
26			14,586	0,474	3,457	1,479
27			13,353	0,659	3,895	1,026
28			4,237	1,073	2,703	1,051
29			3,343	2,738	4,338	1,102
30			9,89	1,287	3,5	1,151
31			6,582	0,681	2,907	1,099
32			5,246	8,6	3,076	1,08
33			8,803	0,853	3,175	1,072
34			6,895	1,618	3,232	0,922
35			5,146	0,481	2,5	0,491
36			5,019	0,443	2,84	0,613
37			4,74	12,732	4,152	0,526
38			8,746	1,133	2,722	0,584
39			5,272	0,745	3,752	0,808
40			12,202	5,057	3,499	1,278
41			7,158	2,009	3,076	0,903
42			2,94	1,757	2,386	0,813
43			9,979	0,423	4,483	1,583
44			6,894	0,477	3,406	0,817
45			3,674	1,544	3,669	0,953
46			10,607	8,117	3,752	1,339
47			3,907	0,312	5,112	0,975
48			4,247	1,788	2,733	0,644
49			18,707	0,706	2,733	0,842
50			11,667	0,679	3,177	0,741
51			9,303	1,146	2,332	0,911
52			6,936	1,23	2,952	1,075
53			6,932	3,012	4,069	0,604
54			4,373	0,86	3,833	0,61
55			5,69	2,235	3,861	0,69
56			7,989	1,452	3,278	1,217
57			1,919	18,118	3,443	0,772
58			3,795	3,097	3,941	0,914
59			3,497	0,984	4,123	0,538
60			2,619	0,674	3,792	0,644
61			3,049	3,389	3,431	0,959
62			8,197	0,631	4,23	0,886
63			3,553	2,422	4,129	0,919
64			5,081	5,499	4,129	1,12
65				0,724	3,226	1,138
66				0,596	2,393	1,192
67				2,1	4,523	1,317
68				1,038	2,17	1,118
69				1,695	3,322	1,081
70				14,199	2,421	1,218
71				7,348	4,653	0,912
72				0,502	3,322	0,745
73				3,602	3,594	0,83
74				0,578	4,667	1,066
75				1,079	4,882	0,9
76				0,912	4,716	1,032
77				1,239	4,977	1,048
78				2,279	5,108	1,238
79				2,196	2,657	0,52
80				1,298	6,475	0,599
81				1,151	3,144	1,31
82				0,514	3,669	1,502
83				0,651	4,128	1,301
84				0,612	3,181	0,979
85				1,686	3,181	0,977
86				0,578	4,745	0,952
87				0,636	5,198	1,322
88				0,665	2,29	1,287
89					3,192	0,884
90					2,761	0,892
91					2,84	0,977
92					2,84	1,051
93					3,099	1,405
94					4,175	1,099
95					2,991	0,877
96					3,467	0,892
97					4,316	0,801
98					4,011	1,31
99					2,883	0,691
100					2,906	1,002

101	3.25	1.065
102	3,126	0,795
103	2.521	1.329
104	1,824	0,658
105	1.766	1.164
106	1.562	1.132
107	2.862	1.388
108	4.366	1.159
109	2.389	1.651
110	3.39	1.365
111	3.765	1.482
112	4.114	1.375
113	1.572	1.598
114	2.132	1.268
115	3.26	1.587
116	3.795	1.656
117	2.491	1.168
118	2.209	1.733
119	5.049	1.651
120	2.156	1.303
121	2.938	1.552
122	2.938	1.175
123	4.905	1.384
124	3.558	1.225
125	5.26	1.025
126	3.033	1.574
127	4.066	1.138
128	3.015	1.275
129	2.967	1.408
130	5.758	1.188
131	2.743	1.077
132	2.502	1.165
133	2.641	1.238
134	3.379	1.15
135	3.09	0.98
136	3.357	0.8
137	3.107	0.801
138	2.245	0.914
139	4.05	0.869
140	2.137	0.952
141	3.703	1.214
142	3.026	1.013
143	2.697	1.506
144	2.015	1.363
145	4.123	0.974
146	2.66	1.262
147	2.745	0.957
148	1.885	1.361
149	3.249	0.933
150	3.819	1.224
151	3.911	1.582
152	2.721	1.153
153	1.93	1.53
154	2.073	1.115
155	2.573	1.678
156	3.436	1.076
157	3.062	1.037
158	4.245	1.368
159	3.359	1.33
160	5.995	1.561
161	3.917	1.031
162	4.772	1.383
163	4.565	0.985
164	4.475	1.42
165	3.469	1.516
166	3.21	1.227
167	3.392	1.616
168	3.954	1.423
169	4.153	1.085
170	4.002	0.996
171	4.03	1.264
172	5	0.865
173	4.066	1.172
174	3.942	1.122
175	1.842	1.02
176	4.189	1.046
177	4.07	1.359
178	2.782	1.408
179	3.233	1.295
180	4.313	1.703
181	1.663	1.836
182	4.72	1.103
183	2.764	1.415
184	3.919	1.393
185	3.387	0.959
186	3.14	1.141
187	4.429	1.148
188	4.17	1.438
189	3.346	1.324
190	3.751	1.536
191	3.108	1.701
192	4.253	1.504
193	3.304	1.121
194	3.155	1.273
195	3.322	1.02
196	3.49	1.096
197	3.297	1.384
198	3.415	1.151
199	3.208	0.951
200	2.985	1.131
201	4.507	1.225
202	2.631	1.509
203	2.383	1.58

204	3,289	1,385
205	4,321	1,383
206	4,987	1,388
207	2,818	1,675
208	4,104	1,703
209	3,193	1,763
210	3,679	1,151
211	2,56	1,309
212	4,589	1,657
213	2,767	1,13
214	2,307	1,156
215	2,647	1,088
216	3,154	1,474
217	5,012	1,968
218		1,58
219		1,164
220		1,432
221		1,511
222		1,662
223		1,093
224		2,038
225		1,949
226		1,415
227		1,197
228		1,512
229		1,637
230		1,916
231		1,513
232		1,746
233		1,365
234		1,609
235		1,387
236		1,251
237		1,3
238		1,197
239		0,907
240		1,437
241		1,727
242		1,833
243		1,584
244		1,852
245		0,944
246		1,285
247		1,42
248		1,296
249		1,384
250		0,945
251		1,318
252		1,525
253		0,797
254		1,069
255		1,338
256		1,383
257		1,013
258		1,275
259		1,314
260		1,384
261		1,165
262		1,069
263		1,221
264		1,401
265		1,353
266		1,203
267		1,238
268		1,383
269		0,987
270		1,655
271		1,085
272		1,1
273		1,428
274		1,395
275		1,025
276		0,688
277		0,884
278		1,148
279		0,65
280		1,051
281		1,497
282		1,294
283		0,764
284		1,279
285		1,296
286		0,82
287		1,278
288		1,001
289		0,839
290		0,979
291		1,285
292		1,872
293		1,139
294		0,791
295		0,958
296		0,763
297		1,169
298		1,026
299		0,607
300		1,039
301		1,339
302		1,204
303		1,113
304		1,315
305		0,861
306		0,946

307						1.035
308						1.106
309						0,947
310						1.001
311						1.275
312						0,731
313						1,509
314						1,072
315						1,347
316						1,328
317						1,107
318						1,16
319						1,117
320						1,1
321						1,556
322						2
323						1,094
324						0,964
325						1,031
326						1,408
327						0,952
328						1,196
329						1,629
330						1,363
331						0,914
332						1,316
333						0,851
334						0,676
335						0,751
336						1,145
337						0,858
338						0,942
339						0,993
340						1,076
341						1,354
342						1,348
343						0,738
344						1,266
345						1,139
346						0,761
347						0,749
348						0,793
349						0,958
350						0,806
351						0,863
352						1,206
353						1,484
354						1,021
355						1,067
356						1,387
357						1,022
Number of data	12	8	64	88	217	357
Max	34,415	53,881	21,561	18,118	6,475	2,038
min	7,485	20,173	0,618	0,312	1,562	0,473
Average	19,67758333	39,239875	7,538265625	2,153284091	3,427847926	1,146890756
SD	8,500068465	11,05637395	4,362485695	2,956801615	0,877730291	0,312411267